

Book of abstracts

MicroNanoFluidics Conference

15th-16th March 2018 in Grenoble

Table of contents

Fluid deposition and spreading on topography, Juel Anne	6
Interface assembly of microcapsules via liquid-liquid droplets templates, Xie Kaili [et al.] .	8
Dynamics of a 2D droplet in a Hele-Shaw cell, Reichert Benjamin [et al.]	9
Cleaning Surfaces from Nanoparticles with Polymer Film: Impact of Polymer Removal Conditions, Lallart Adeline [et al.]	11
2.5D Nanofluidics: Grayscale Laser Lithography and Two Phase Flow in Non-Uniform Depth Nanochannels, Naillon Antoine [et al.]	13
The microfluidic laboratory at the Synchrotron SOLEIL, Mateo Tiphaine [et al.]	15
Self-similar relaxation of a confined non-wetting droplet, Kerdraon Margaux [et al.]	16
The sliding walls: a new toolbox for manually-operated microfluidic, Venzac Bastien [et al.]	17
Transport of emulsions in heterogeneous environment, Le Blay Marine [et al.]	18
Adsorption-Induced Slip Inhibition for Polymer Melts on Ideal Substrates, McGraw Joshua [et al.]	19
Dynamical study of confined bubbles in cylindrical capillary tubes submitted to a Marangoni stress, Mansur Alexandre	20
Soap films for gas separation, Hadji Celine [et al.]	21
Fabrication of clamped-clamped microbeams with embedded nanochannels towards nanoparticles sensing, Scaiola Davide [et al.]	23
Liquid phase exfoliation of graphene in hydrocavitating labs-on-a-chip, Qiu Xiaoyu [et al.]	24
Transport of nano-objects in narrow channels: influence of Brownian diffusion, confinement and particle nature, Liot Olivier [et al.]	25
Ultrasound transmission through microfluidics-generated liquid foams, Champougny Lorène [et al.]	27
Using Microfluidic as a Tool for Biological Macromolecular Serial Crystallography on a Synchrotron Beamline : Proxima-1, Chaussavoine Igor	28
Self-cleaning slippery infused surfaces for dairy processing, Thomy Vincent [et al.]	29
Laboratoire sur puce pour la détection d'événements cellulaires rares, Valette Marion [et al.]	30
Bottom-up assembly of cells in flow with dielectrophoresis, Cottet Jonathan	31
The Physics and Engineering of Active Matter, Di Leonardo Roberto	33
Dynamics of fibers transported in confined viscous flow, Cappello Jean [et al.]	35
Deformability-based (micro)fluidic sorting, Le Goff Anne [et al.]	36
Direct measurement of liquid flow rate up to picoliter per minute, Sharma Preeti [et al.] .	38
Active sieving : from flapping nano-doors to vibrating nanotubes, Marbach Sophie [et al.]	39
Thermo-osmosis: is it possible to desalinate water using thermal gradients?, Fu Li [et al.]	41

Viscosity of supercooled water and two-state interpretation of water anomalies, Issenmann Bruno [et al.]	42
From microfluidic technology to organ-on-a-chip platfroms: new opportunities to develop physiologically relevant in vitro models, Le Gac Séverine	44
DEVELOPMENT OF A MICROFLUIDIC BIOMIMETIC DEVICE FOR TRIPLE NEGATIVE BREAST CANCER STEM CELLS EXTRAVASATION STUDIES, Treizebre Anthony	46
Microfluidic platform to restore the angiogenic balance in preeclampsia, Alexandre Lucile [et al.]	47
Microbes under pressure, Holt Liam [et al.]	48
On-chip Flow Cell Sorting System Based on High frequency Dielectrophoresis implemented on CMOS technology, Manczak Rémi [et al.]	49
Simple optimization of single-level particle trapping flow-through microfluidic devices using oblique hydrodynamic flow, Fattaccioli Jacques [et al.]	50
Monolithic fabrication of glass suspended microchannel resonator for enhanced biosensing application, Calmo Roberta [et al.]	52
Fluid-particle coupling induced micro-magnetic trapping of highly diffusive magnetic nanoparticles, Fratzl Mario [et al.]	53
PRODUCTION OF BIOSOURCED FOAMS BY MICROCHANNELS AT HIGH THROUGH-PUT, Sepulveda Julian [et al.]	54
Utilizing a Molecular Program for the Hypersensitive Detection of Nucleic Acids, Menezes Roberta [et al.]	55
Active matter in complex media, Brun-Cosme-Bruny Marvin	57
In-situ photo-patterning of pressure-resistant hydrogel membranes with controlled permeabilities in PEGDA microfluidic channels, Keita Camille [et al.]	58
Portable microfluidics based on hyperelastic materials, Parent Charlotte [et al.]	59
Biomimetic Capture of Odorant Molecules in a Microfluidic Device, Tulukcuoglu Guneri Ezgi [et al.]	60
Microfluidic standardization: a status, Verplanck Nicolas [et al.]	61
Microfluidic devices and systems for bio-mimic stem cell processing, Chen Yong	62
Microcapsule fabrication by membrane emulsification, Maleki Mehdi	63
Drying of a water-filled channel within an artificial leaf, Dollet Benjamin [et al.]	65
Dropbox : an "off-the-shelf" microfluidic device for monodisperse emulsification based on a 3D-printed nozzle injector, Dewandre Adrien	66
Light propelled thermocapillary vessel, Dutour Thomas [et al.]	67
Experimental study on acetone vapor as the tracer molecule for molecular tagging thermometry in gas microflows, Yeachana Varun [et al.]	69
Dynamics and dissolution of bubbles in microchannels, Rivero-Rodriguez Javier [et al.] . .	70
Cavitating flow in microchannels : thermal effects and chemiluminescence., Colombet Damien [et al.]	71
Study of flow properties of foam in model porous media, Mauray Alexis [et al.]	72
Whispering gallery mode yields intense acoustic streaming in sessile droplets, Riaud Antoine [et al.]	73
List of participants	74
List of exhibitors	75
Author Index	76

Thursday, March 15, 2018

TIME	EVENT
09:00 - 09:30	Welcome reception - Welcome reception
09:30 - 10:15	Invited conference
09:30 - 10:15	› Fluid deposition and spreading on topography - <i>Anne Juel, University of Manchester</i>
10:15 - 10:55	Drops, bubbles, etc ...
10:15 - 10:35	› Interface assembly of microcapsules via liquid-liquid droplets templates - <i>Kaili Xie, Laboratoire de Mécanique, Modélisation et Procédés Propres, Laboratoire Rhéologie et Procédés - Clement de Loubens, Laboratoire Rhéologie et Procédés (LRP)</i>
10:35 - 10:55	› Dynamics of a 2D droplet in a Hele-Shaw cell - <i>Benjamin Reichert, Gulliver</i>
10:55 - 11:25	Coffee break
11:25 - 12:05	Microfabrication
11:25 - 11:45	› Cleaning Surfaces from Nanoparticles with Polymer Film: Impact of Polymer Removal Conditions - <i>adeline Lallart, Laboratoire des écoulements géophysiques et industriels, Laboratoire Interdisciplinaire de Physique [Saint Martin d'Hères], STMicroelectronics</i>
11:45 - 12:05	› 2.5D Nanofluidics: Grayscale Laser Lithography and Two Phase Flow in Non-Uniform Depth Nanochannels - <i>Antoine Naillon, LAAS-CNRS, Institut de mécanique des fluides de Toulouse, Laboratoire Rhéologie et Procédés</i>
12:05 - 12:30	Poster flash presentations
12:05 - 12:06	› The microfluidic laboratory at the Synchrotron SOLEIL - <i>Tiphaine Mateo, Synchrotron SOLEIL - Benedikt Lassalle, Synchrotron SOLEIL</i>
12:06 - 12:08	› Self-similar relaxation of a confined non-wetting droplet - <i>Margaux Kerdraon, MMN, Gulliver</i>
12:08 - 12:09	› The sliding walls: a new toolbox for manually-operated microfluidic - <i>Bastien Venzac, Institut Curie</i>
12:09 - 12:11	› Transport of emulsions in heterogeneous environment - <i>Marine LE BLAY, Laboratoire de Physique de IÉNS Lyon</i>
12:11 - 12:12	› Adsorption-Induced Slip Inhibition for Polymer Melts on Ideal Substrates - <i>Joshua McGraw, Département de Physique, Ecole Normale Supérieure</i>
12:12 - 12:14	› Dynamical study of confined bubbles in cylindrical capillary tubes submitted to a Marangoni stress - <i>Alexandre Mansur, Gulliver, ESPCI ParisTech</i>
12:14 - 12:15	› Soap films for gas separation - <i>Celine Hadji, Laboratoire Interdisciplinaire de Physique [Saint Martin d'Hères]</i>
12:15 - 12:17	› Fabrication of clamped-clamped microbeams with embedded nanochannels towards nanoparticles sensing - <i>Davide Scaiola, DISAT - Politecnico di Torino, EPFL-STI-IMT-LMIS4</i>
12:17 - 12:18	› Liquid phase exfoliation of graphene in hydrocavitating labs-on-a-chip - <i>Xiaoyu Qiu, LEGI</i>
12:18 - 12:20	› Transport of nano-objects in narrow channels: influence of Brownian diffusion, confinement and particle nature - <i>Olivier Liot, Institut Lumière Matière</i>
12:20 - 12:21	› Ultrasound transmission through microfluidics-generated liquid foams - <i>Lorène Champougny, Gulliver</i>
12:21 - 12:23	› Using Microfluidic as a Tool for Biological Macromolecular Serial Crystallography on a Synchrotron Beamline : Proxima-1 - <i>Igor Chaussavoine, Proxima-1 Synchrotron SOLEIL</i>
12:23 - 12:24	› Self-cleaning slippery infused surfaces for dairy processing - <i>vincent Thomy, Institut d'électronique, de microélectronique et de nanotechnologie, University of Lille Nord de France, Institute of Electronics, Microelectronics and Nanotechnology</i>
12:24 - 12:26	› Laboratoire sur puce pour la détection d'événements cellulaires rares - <i>Anne-Marie Gué, Laboratoire d'analyse et d'architecture des systèmes [Toulouse]</i>

TIME	EVENT
12:26 - 12:28	› Bottom-up assembly of cells in flow with dielectrophoresis - <i>Jonathan Cottet, Laboratoire de Microsystèmes 4 (LMIS4), Laboratoire Ampère (Ampère)</i>
12:30 - 14:30	Lunch & posters
14:30 - 15:15	Invited conference
14:30 - 15:15	› The Physics and Engineering of Active Matter - <i>Roberto Di Leonardo, Dipartimento di Fisica [Roma La Sapienza]</i>
15:15 - 15:55	Drops, bubbles, etc ...
15:15 - 15:35	› Dynamics of fibers transported in confined viscous flow - <i>Jean Cappello, Physique et mécanique des milieux hétérogènes</i>
15:35 - 15:55	› Deformability-based (micro)fluidic sorting - <i>Anne Le Goff, Biomécanique et Bioingénierie</i>
15:55 - 16:25	Coffee break
16:25 - 17:45	Nanofluidic
16:25 - 16:45	› Direct measurement of liquid flow rate up to picoliter per minute - <i>Preeti Sharma, Laboratoire Interdisciplinaire de Physique [Saint Martin d'Hères]</i>
16:45 - 17:05	› Active sieving : from flapping nano-doors to vibrating nanotubes - <i>Sophie Marbach, Ecole Normale Supérieure</i>
17:05 - 17:25	› Thermo-osmosis: is it possible to desalinate water using thermal gradients? - <i>Li FU, Institut Lumière Matière</i>
17:25 - 17:45	› Viscosity of supercooled water and two-state interpretation of water anomalies - <i>Bruno Isenmann, Institut Lumière Matière - Université Lyon 1</i>
19:30 - 23:00	Dinner

Friday, March 16, 2018

TIME	EVENT
09:10 - 09:55	Invited conference
09:10 - 09:55	› From microfluidic technology to organ-on-a-chip platfroms: new opportunities to develop physiologically relevant in vitro models - <i>Séverine Le Gac, University of Twente</i>
09:55 - 10:55	Lab On Chip
09:55 - 10:15	› Development of a microfluidic biomimetic device for triple negative breast cancer stem cells extravasation studies - <i>Anthony TREIZEBRE, Institut d'Électronique, de Microélectronique et de Nanotechnologie (IEMN) - UMR 8520</i>
10:15 - 10:35	› Microfluidic platform to restore the angiogenic balance in preeclampsia - <i>Lucile Alexandre, Institut Pierre-Gilles de Gennes pour la Microfluidique, Sorbonne Universités, Institut Curie</i>
10:35 - 10:55	› Microbes under pressure - <i>Morgan Delarue, Laboratoire d'analyse et d'architecture des systèmes [Toulouse]</i>
10:55 - 11:25	Coffee break
11:25 - 12:05	Lab On Chip
11:25 - 11:45	› On-chip Flow Cell Sorting System Based on High frequency Dielectrophoresis implemented on CMOS technology - <i>Arnaud Pothier, XLIM</i>
11:45 - 12:05	› Simple optimization of single-level particle trapping flow-through microfluidic devices using oblique hydrodynamic flow - <i>Jacques FATTACCIOLI, Département de Chimie</i>
12:05 - 12:30	Poster flash presentations

TIME	EVENT
12:05 - 12:06	› Monolithic fabrication of glass suspended microchannel resonator for enhanced biosensing application - <i>Roberta Calmo, Politecnico di Torino [Torino]</i>
12:06 - 12:08	› Fluid-particle coupling induced micro-magnetic trapping of highly diffusive magnetic nanoparticles - <i>Mario Fratzl, Institut Néel, Laboratoire de Génie Electrique de Grenoble</i>
12:08 - 12:09	› Production of biosourced foams by microchannels at high throughput - <i>Julian Sepulveda, Université de Nantes</i>
12:09 - 12:11	› Utilizing a Molecular Program for the Hypersensitive Detection of Nucleic Acids - <i>Roberta Menezes, Université Paris Descartes & ESPCI ParisTech</i>
12:11 - 12:12	› Active matter in complex media - <i>Marvin Brun-Cosme-Bruny, Marvin Brun-Cosme-Bruny</i>
12:12 - 12:14	› In-situ photo-patterning of pressure-resistant hydrogel membranes with controlled permeabilities in PEGDA microfluidic channels - <i>Camille KEITA, CNRS-SOLVAY</i>
12:14 - 12:15	› Portable microfluidics based on hyperelastic materials
12:15 - 12:17	› Biomimetic Capture of Odorant Molecules in a Microfluidic Device - <i>Ezgi TULUKCUOGLU GUNERI, CEA LETI MINATEC Campus, Univ. Grenoble F-38054 Grenoble, France</i>
12:17 - 12:18	› Microfluidic standardization: a status - <i>Nicolas Verplanck, CEA-LETI</i>
12:18 - 12:20	› Microfluidic devices and systems for bio-mimic stem cell processing - <i>Yong Chen, Ecole normale supérieure</i>
12:20 - 12:21	› Microcapsule fabrication by membrane emulsification - <i>Mehdi Maleki, MALEKI Mehdi</i>
12:21 - 12:23	› Drying of a water-filled channel within an artificial leaf
12:23 - 12:24	› Dropbox : an "off-the-shelf" microfluidic device for monodisperse emulsification based on a 3D-printed nozzle injector - <i>Adrien Dewandre, Université Libre de Bruxelles [Bruxelles]</i>
12:24 - 12:26	› Light propelled thermocapillary vessel - <i>Cyril Picard, Laboratoire Interdisciplinaire de Physique [Saint Martin d'Hères]</i>
12:30 - 14:30	Lunch & posters
14:30 - 16:10	Drops, bubbles, etc ...
14:30 - 14:50	› Experimental study on acetone vapor as the tracer molecule for molecular tagging thermometry in gas microflows - <i>Varun Yeachana, Institut Clément Ader (ICA), Université de Toulouse, CNRS, INSA, ISAE-SUPAERO, Mines-Albi, UPS, Toulouse France</i>
14:50 - 15:10	› Dynamics and dissolution of bubbles in microchannels - <i>Javier Rivero-Rodriguez, Transferts, Interfaces et Procédés - Physique des fluides, Université Libre de Bruxelles</i>
15:10 - 15:30	› Cavitating flow in microchannels : thermal effects and chemiluminescence. - <i>Damien Colombet, Laboratoire des écoulements géophysiques et industriels</i>
15:30 - 15:50	› Study of flow properties of foam in model porous media - <i>Alexis Mauray, Laboratoire Rhéologie et Procédés</i>
15:50 - 16:10	› Whispering gallery mode yields intense acoustic streaming in sessile droplets - <i>Antoine Riaud, Institut d'électronique, de microélectronique et de nanotechnologie, Institut des Nanosciences de Paris</i>

Invited conference (I)

Fluid deposition and spreading on topography

A. Juel^a

^aManchester Centre for Nonlinear Dynamics and School of Physics & Astronomy, University of Manchester, UK

Microdroplet deposition is a technology that spans applications from tissue engineering to microelectronics. Our high-speed imaging measurements reveal how sequential linear deposition of overlapping droplets on flat uniform substrates leads to striking non-uniform morphologies for moderate contact angles. We develop a simple physical model, which for the first time captures the post-impact dynamics drop-by-drop: surface-tension drives liquid redistribution, contact-angle hysteresis underlies initial non-uniformity, while viscous effects cause subsequent periodic variations. Motivated by applications to the manufacture of POLED displays, we turn to the spreading of a single droplet within a recessed stadium-shaped pixel. We find that the sloping side wall of the pixel can either locally enhance or hinder spreading depending on whether the topography gradient ahead of the contact line is positive or negative. Locally enhanced spreading occurs via the formation of thin pointed rivulets along the side walls of the pixel through a mechanism similar to capillary rise in sharp corners. We demonstrate that a thin-film model combined with an experimentally measured spreading law, which relates the speed of the contact line to the contact angle, provides excellent predictions of the evolving liquid morphologies of multiple-droplet deposits on topography.

Drops, bubbles, etc ... (I)

Interface assembly of microcapsules via liquid-liquid droplets templates

Kaili. Xie^{a,b}, Clément de Loubens^b, Frédéric Dubreuil^c, Marc Leonetti^b

^aAix-Marseille Université, CNRS, Centrale Marseille, M2P2 UMR7340, Marseille, France

^bUniv. Grenoble Alpes, CNRS, Grenoble INP, LRP UMR 5520, Grenoble, France

^cUniv. Grenoble Alpes, CNRS, Cermav, Grenoble, France

Key words: microcapsule, water-in-oil emulsion, shell instability

1. Introduction

In the advanced drug delivery and release systems, isolation and protection of the core ingredients from the complicatedly and brutally external environment is often an essential step.[1] Microcapsules recently are accepted as versatile tools to achieve such objectives, have boomed greatly. However, fabrication and mechanical properties tuning of microcapsules through a cost-efficient route are still two challenging aspects. Here, we propose a facile method of assembling capsules shell by taking advantage of two oppositely charged ingredients naturally, via the liquid-liquid droplets templates produced by microfluidic technique. [2] The capsules shells are formed by adding negatively charged surfactant, phosphatidic acid (PFacidYN) around liquid droplets templates filled with positively charged polysaccharid (chitosan). Controlling of the shell complexation time and concentrations of PFacidYN and chitosan allows us to tune the shell properties in a large range which could satisfy various using purposes. We utilize a millimetric cross-slot flow cell to characterize the shell properties,[3] including interfacial rheology and shell instability.

2. Results

A T-junction microfluidic chip is used to make the liquid-liquid droplets templates, as shown in figure1(a). Thanks to the flow rates of two immiscible phases well controlled in microfluidic systems, the size distribution is within 5%, in figure1(b). Surface shear elastic modulus of interface is measured based on the small deformation theory, in figure1(c). Since the thickness of capsule shell, $h \ll R$, where R is radius of capsule, shell instability happens when the total energy is sufficiently large that induces the thin shell bending out of the surface. And the critical buckling state has been studied experimentally.

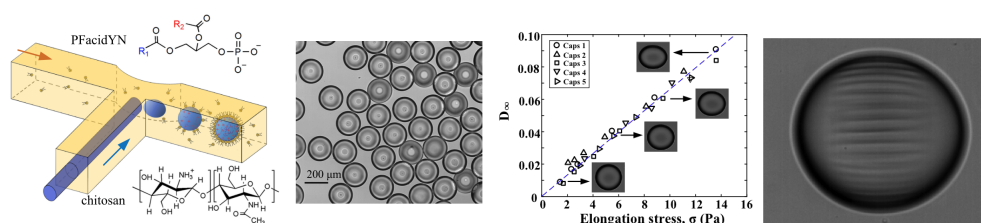


Figure 1: From left to right: (a) liquid-liquid droplets generated in T-junction chip; (b) monodisperse capsules on substrate; (c) Capsules steady-state deformation with elongation stress; (d) shell instability

References

- [1] J. L. Markman, A. Rekechenetskiy, E. Holler, et. al., Nanomedicine therapeutic approaches to overcome cancer drug resistance, *Adv. Drug. Deliv. Rev.*, 65, 1866-1879 (2013).
- [2] K. Xie, C. de Loubens, F. Dubreuil, et. al., Interfacial rheological properties of self-assembling biopolymer microcapsules, *Soft Matter*, 13, 6208-621765 (2017).
- [3] C. de Loubens, J. Deschamps, G. Boedec, et. al., Stretching of capsules in an elongation flow, a route to constitutive law, *Journal of Fluid Mechanics*, 767, R3:1-11 (2015).

Dynamics of a 2D droplet in a Hele-Shaw cell

B. Reichert^a, A. Huerre^a, O. Theodoly^b, I. Cantat^c and Marie-Caroline Jullien^a

^a*Gulliver UMR CNRS 7083, ESPCI Paritech, 10 rue Vauquelin, 75005 Paris, France*

^b*LAI, INSERM UMR 1067, CNRS UMR 7333, Aix-Marseille Université 13009 Marseille, France*

^c*IPR, UMR CNRS 6251, Université Rennes 1 35042 Rennes, France*

Key words: droplet, Hele-Shaw cell, lubrication film, interface

Droplet microfluidics is a growing field of research. However, the dynamics of these objects remain misunderstood. Indeed, a question as fundamental as predicting the droplet velocity while pushed by an external fluid at a given velocity (Fig.1) is still not answered [1] [2]. Understanding the dynamics of a droplet requires characterizing the viscous dissipation mechanisms (friction) within the droplet and in the lubrication film. As this dissipation is related to the geometry and to the physicochemical properties of the interface separating the inner phase of the droplet from the outer phase, predicting a droplet velocity requires determining both the lubrication film topography and the boundary condition at the interface.

This work presents a characterization of the dynamics of 2D droplets in a Hele-Shaw cell (Fig. 1), by taking advantage of the double measurement of the lubrication film profile by interference microscopy [3] and of the droplet velocity. We consider fluorinated oil droplets in an aqueous solution containing C₁₀TAB above the CMC (990 mM) and NaCl at 1 M to screen the electrostatic interactions (Fig. 2). Interestingly, in the central axis of droplet migration, the lubrication film is recovered at the front considering a stress-free boundary condition, while the rear meniscus requires a rigid boundary condition. This is the signature that the surfactant surface concentration is not homogeneous along the interface and accumulates at the rear. The measured profile allows extracting the boundary condition at the interface (interfacial velocity and corresponding surface tension gradient). Furthermore, in a transverse direction, the profile displays a vault shape that can be modeled considering a Bretherton [4] like model, involving the normal velocity to the contour of the droplet.

In a second part, it is possible to calculate the dissipation in each part of the lubrication film thanks to the profiles that have been previously described. We present a model that allows to reproduce the droplet velocity without any fitting parameter, by considering the different boundary conditions from the front meniscus to the rear one. We show that the model is very sensitive to the local boundary condition at the interface. This result clearly shows that predicting droplet velocity calls for the knowledge of the local boundary condition at the interface that is likely to be altered by the presence of surfactants.

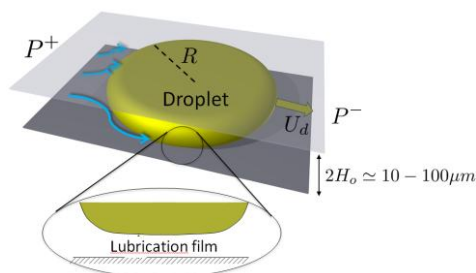


Fig.1 Squeezed droplet in a Hele-Shaw cell

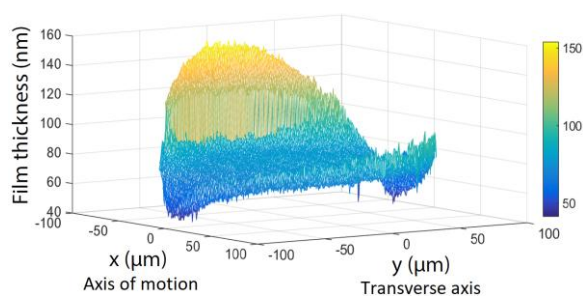


Fig.2 Experimental topography of the lubrication film

References

- [1] G. Taylor, P.G. Saffman, A note on the motion of bubbles in a Hele-Shaw cell and porous medium, *The Quarterly Journal of Mechanics and Applied Mathematics*, 12, 265-279 (1959)
- [2] C-W Park, S. R.K. Maruvada, The influence of surfactant on the bubble motion in Hele-Shaw cells, *Phys. Fluids*, 6, 3267-3275 (1994)
- [3] A. Huerre, M.-C. Jullien, O. Theodoly and M.-P. Valignat, *Lap on a chip*, 16, 911-916 (2016)
- [4] F. P. Bretherton, The motion of long bubbles in tubes, *J. Fluid Mech.*, 10, 166-188 (1961)

Microfabrication

Cleaning Surfaces from Nanoparticles with Polymer Film: Impact of Polymer Removal Conditions

A. Lallart^{a,b,c}, P. Garnier^a, E. Lorenceau^b, A. Cartellier^c, E. Charlaix^b

^a*STMicroelectronics Crolles2, 850 rue Jean Monnet 38921 Crolles, France*

^b*Univ. Grenoble Alpes, CNRS, LIPhy, 38000 Grenoble, France*

^c*Univ. Grenoble Alpes, Grenoble INP, LEGI, 38000 Grenoble, France*

Key words: Nanoparticles, Particle removal, Polymer, Centrifugal force

1. Introduction

In order to keep a high yield during integrated circuits production, a continuous improvement has been carried out in the particles cleaning area, switching from brushes and acoustic cleans to high velocity sprays. Moreover, as typical dimension of microelectronic circuit are getting smaller and smaller, tinier and tinier particles have to be removed (Figure 1). Even though the adhesion and removal of particles on solid surfaces have been studied and documented for years, the integrated circuits industry still misses robust solutions to clean nanoparticles, keeping finest transistors features integrity, and extremely low material consumption [1].

Recently, it has been shown that new processes involving non-Newtonian fluid enable an excellent nanoparticles removal without features damage [2]. In this process, a thin layer of a well-chosen polymer is deposited on the nanoparticles contaminated wafer. Then, the polymer is removed either by peeling or by an extensional flow. To understand the remarkable ability of polymer to remove nanoparticles, two mechanisms are postulated. In the peeling process, the removal capacity is based on a better adhesion between the particles and the polymer rather than between the particles and the surface [2]. In the extensional flow system, the polymer is kept in a liquid state and removed by a siphoning action and the particles are withdrawn from the surface thanks to the fluid viscoelastic properties [3]. Even though they are quite convincing, these two mechanisms still need to be validated by experimental studies in particular when the polymer used to remove the nanoparticles is not truly a liquid or a solid but a viscoelastic liquid exhibiting a complex rheology.

2. Experimental

Silicon wafers of 300 mm diameter are intentionally contaminated by 60nm silica particles. Then, they are coated with a polymer layer. This latter is spray stripped with a chemical solution and the cleaning efficiency of the process is quantified by counting nanoparticles before and after the complete polymer removal step thanks to a KLA Surfscan SP3 blue laser diffraction tool.

3. Results & Discussion

In our work, the polymer layer is removed using a spray dispense with centrifugation rather than siphoning. This process enables a high particle removal efficiency up to 90 % in average. However, the efficiency is not homogeneous: as can be seen in Table 1, the particles removal efficiency is very high far from the spray injection while a lower efficiency is observed in the vicinity of the spray injection.

To understand these observations, we focus on the influence of wafer centrifugation and viscoelastic properties of the polymer layer. By writing a stress balance on the polymer layer, we have been able to establish a correlation between the viscoelastic properties of the polymer,

measured thanks to a cone-plan rheometer, and the centrifugal force, which exert an external force on the polymer layer.

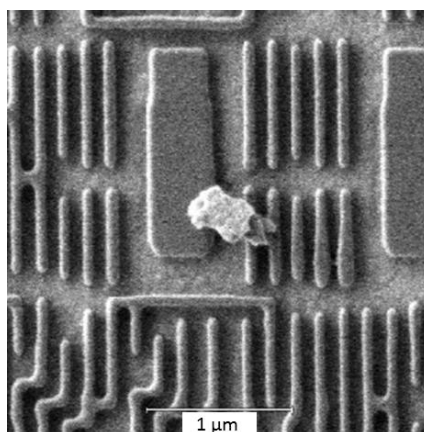


Figure 1: Particle on a patterned surface

	Initial Contamination	Post Process Polymer A	Post Process Polymer B
Mapping Defects > 30nm			
Removal Efficiency		82 %	90 %

Table 1: Efficiency of the cleaning process depending on the polymer layer

References

- [1] B.K. Kirkpatrick, and al., "Material Loss Impact on Device Performance for 32nm CMOS and Beyond", Solid State Phenomena, 145-146, pp. 245-248 (2009)
- [2] P. Lin, S. Pi, H. Jiang, and Q. Xia, "Mold cleaning with polydimethylsiloxane (PDMS) for nanoimprint lithography," Nanotechnology, vol. 24, no. 32 (2013)
- [3] T. Walker and T. Hsu, "Enhanced particle removal using viscoelastic fluids," J. Rheol. (N. Y. N. Y), vol. 58, no. 1, pp. 63–88 (2014)

2.5D Nanofluidics: Grayscale Laser Lithography and Two Phase Flow in Non-Uniform Depth Nanochannels

A. Naillon^{a,b,c}, M. Prat^b, P. Joseph^c

^aUniversité Grenoble Alpes, LRP, Grenoble, France

^bInstitut de Mécanique des Fluides de Toulouse-Université de Toulouse, CNRS-INPT-UPS, Toulouse, France

^cLAAS-CNRS, Université de Toulouse, CNRS, Toulouse, France

Key words: nanofluidics, nanofabrication, grayscale laser lithography, direct writing, imbibition, drainage.

Standard micro and nanofabrication techniques naturally lead to planar structures made of a succession of flat sheets. However, devices including relief in their structures lead to new functionalities in many application fields by opening the path to topologies not accessible in 2D. In this work, we report a versatile method to fabricate silicon–glass nanofluidic chips with non-uniform channel depths in the range 20-500 nm and micrometer resolution in width. It is based on a single step of grayscale laser lithography and reactive ion etching [1]. Complex structures are fabricated such as slopes, step channels or pore networks that mimic nanoporous media (Fig. 1a).

In order to demonstrate the accuracy of our process, the kinetics of imbibition in straight nanochannels with non-uniform depth is measured and compared with a theoretical model (Fig. 1b). Quantitative agreement is obtained. Nevertheless, it is reported bubble trappings due to the thickening of corner liquid films at each crossing step.

Then, the method is used to fabricate a network of interconnected slits of non-uniform depth, a geometry mimicking a nanoporous medium in which a pressure step-controlled drainage experiment is performed, i.e., the immiscible displacement of a wetting fluid (liquid water) by a non-wetting one (nitrogen). The drainage patterns are analysed by comparison with simulations based on the invasion percolation algorithm (Fig.1c). The results indicate that slow drainage in the considered nanofluidic system well corresponds to the classical capillary fingering regime.

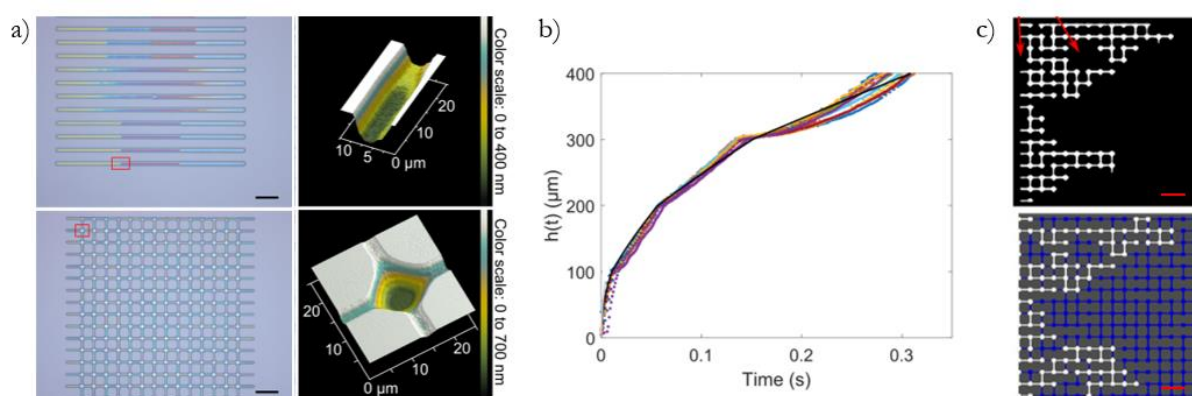


Figure 1: a) Picture after grayscale laser lithography and AFM image after etching. Top: varying depth nanochannels and zoom on a step. Bottom: pore network and zoom on a pore. b) Experimental (colored dots) and theoretical (black line) imbibition kinetics in a four steps nanochannel. c) Comparison between experiment (top) and pore network simulation (bottom) during the drainage of a 2.5D nanopore network. Red arrows point liquid cluster. Scale bar represents 50 μm .

References

[1] Naillon et al., "Quasi-static drainage in a network of nanoslits of non-uniform depth designed by grayscale laser lithography", *Microfluidics and Nanofluidics*, 21, 131 (2017)

Posters (I)

The microfluidic laboratory at the Synchrotron SOLEIL

T. Mateo, I. Chaussavoine, S. Lefrançois, Y. Liatimi, T. Bizien, L. Chavas, B. Lassalle-Kaiser.
Synchrotron SOLEIL, l'Orme des Merisiers, 91192, Gif-sur-Yvette.

Key words: Synchrotron radiation, Crystallography and Spectroscopy

1. Introduction

Synchrotrons offer a wide range of photon-based techniques, which outcompete tabletop instruments that can be found in a laboratory. These techniques are as varied as spectroscopy, diffraction, diffusion or imaging, using photons ranging from the IR to Hard X-rays, through UV and soft X-rays. A microfluidic laboratory has recently opened at SOLEIL, the French national synchrotron source, with the aim to combine advanced photon techniques with microfluidic tools. Applications in protein crystallography, physico-chemistry of interfaces and nanoparticles synthesis are expected on the short term.

2. Laboratory description and upcoming projects

The microfluidic laboratory of SOLEIL aims at providing the environment, the tools and the expertise for users to develop original research projects that combine synchrotron-based techniques and microfluidics. A 25m² clean room and a 20m² shop is available for users. The cleanroom features all the equipment required for the preparation of microfluidic chips by soft lithography (spincoater, insulating device, laserwriter, profilometer), while the shop has a 3D-printer, pressure controller and microscopes for device testing.

We are currently working on the three following projects:

- i) The development of microfluidic traps for the immobilization of micron-sized protein crystals and their subsequent study by X-ray diffraction. This method allows studying protein crystals at room temperature and under “friendly” conditions as compared to cryogenic conditions. This project is led by Leonard Chavas from the Proxima-1 beamline.
- ii) Microfluidic mixers are being developed for the time-resolved study of protein folding processes and nanoparticle synthesis using small angle X-ray scattering (SAXS). This work is carried out by the team of the SWING beamline.
- iii) Microfluidic electrochemical cells are also being developed, with the final aim of performing sequential CO₂ reduction reaction. Along the course of this multi-step reaction, we will probe the structural and electronic evolution of electrocatalysts by using *in situ* or *operando* X-ray absorption spectroscopy. This work is led by Benedikt Lassalle and carried out on the ROCK and SAMBA beamlines.

We will show the advances made in these three projects and propose new upcoming ones.

Self-similar relaxation of a confined non-wetting droplet

Margaux Kerdraon^a, Joshua D. McGraw^a, Stéphanie Descroix^b, Marie-Caroline Jullien^a

^a*Gulliver, ESPCI 10 rue vanquelin, 75005 PARIS*

^b*MMBM, Institut Curie, 6 rue Jean Calvin, 75005 PARIS*

Key words: Relaxation, non-wetting confined droplet, self-similarity

Despite the growing field of droplet-based microfluidics, few theoretical tools are available to describe 3D flows in confined droplets in square or rectangular channels. Furthermore, few model experiments for such flow situations have been realized. In this study, we experimentally observe the relaxation of a mineral oil droplet in water. The droplet is confined in the rectangular channel of a PDMS microfluidic system. The droplet deformation is induced by the heating of a localized micro-patterned resistance. This heating induces a spontaneous flow such that a neck is formed in the region near the resistance. For the purposes of this study, such a deformation process allows us to prepare a well-defined initial condition for the observed relaxations. These relaxations are driven by Laplace pressure gradients and are mediated by viscous dissipation. We observe that the profile of the neck is self-similar at the late stages and we propose a drainage model that recovers the experimentally observed scaling exponents. The model is based on scaling arguments that take into account both the Laplace pressure generated by the neck and viscous dissipation in the gutters through which the fluid escapes to the unconfined regions of the microfluidic chip. We show that theoretical tools that are classically used such as lubrication equations have to be amended due to the complexity of both the interface shape and the 3D velocity profile.

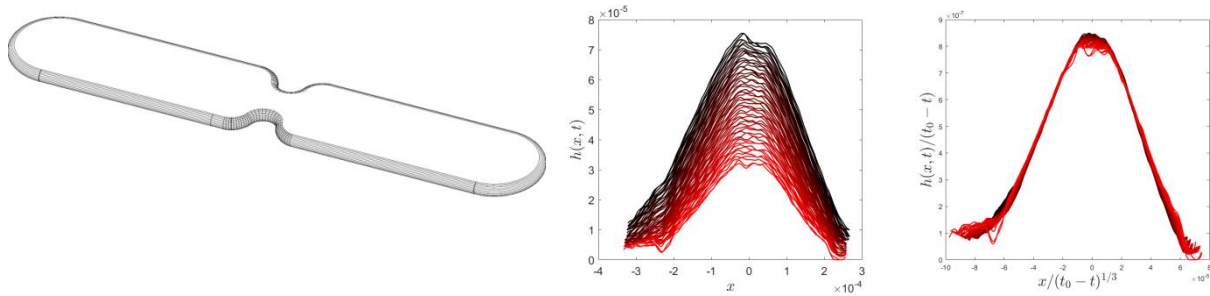


Figure 1: 1) Configuration of the confined non-wetting droplet, 2) Profile of the interface of the droplet during relaxation, 3) Self-similarity of the interface profile.

THE SLIDING WALLS: A NEW TOOLBOX FOR MANUALLY-OPERATED MICROFLUIDIC

B. Venzac^{a,b,c}, Y. Liu^{a,b,c}, I. Ferrante^{a,b,c}, A. Yamada^{a,b,c}, P. Vargas^{b,c,d}, M. Verhulsel^{a,b,c}, L. Malaquin^e, J.-L. Viovy^{a,b,c} and S. Descroix^{a,b,c}

^a*Laboratoire Physico-Chimie Curie, Institut Curie, PSL Research University, CNRS UMR168, FRANCE*

^b*Sorbonne Universités, UPMC Univ Paris 06, FRANCE*

^c*Institut Pierre-Gilles de Gennes, Paris, France*

^d*UMR 144, Institut Curie, PSL Research University, FRANCE*

^e*EliA group, LAAS CNRS, Toulouse, France*

Microfabrication – Manual actuation – Valves – Cell culture – Sample preparation

1. Introduction

The fields of biology and biotechnologies are increasingly interested in microfluidics but spreading of this technology is still limited by the need of external equipment or by technical skills for fluidic operations and microfabrication. Manually-actuated microfluidics is a way to simplify the use of microfluidic systems [1-2]. However, only simple tasks could be manually performed; a versatile technology enabling manual change in channel configuration while being easily implemented in existing microfluidic design is still lacking. We propose the sliding wall technology as a new toolbox to answer this need while performing new operations.

2. Fabrication

A rigid structure is inserted inside a PDMS channel called guiding channel (see Figure 1). This channel intersects fluidic channels, and manual sliding of the rigid structure inside the guiding channel allows the modification of the fluidic network without any external equipment. Several materials and processes were successfully applied for the sliding wall microfabrication, including micro-milling of metallic sheet, soft lithography of NOA81 or stereolithographic 3D printing.

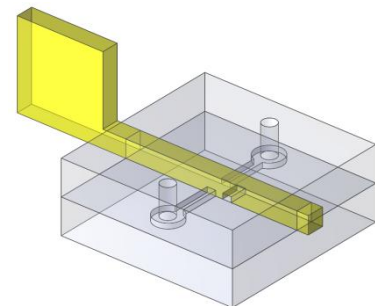


Figure 1: Sliding wall principle.

3. Applications

We have demonstrated a wide range of functionalities:

- ON/OFF valves and two-way valves withstanding up to 400 mbar.
- Manual sample loading and pumping with a minimal dead volume.
- Compartmentalization of large chambers for user-friendly 3D cell culture and migration assay of dendritic cells.
- Sample preparation with an electrophoretic preconcentration and purification of DNA.

References

- [1] M. Oono, K. Yamaguchi, A. Rasyid, A. Takano, M. Tanaka and N. Futai, Reconfigurable microfluidic device with discretized sidewall, *Biomicrofluidics*, 11, 34103 (2017).
- [2] A. Yamada, R. Renault, A. Chikina, B. Venzac, I. Pereiro, S. Coscoy, M. Verhulsel, M. C. Parrini, C. Villard, J.-L. Viovy and S. Descroix, Transient microfluidic compartmentalization using actionable microfilaments for biochemical assays, cell culture and organs-on-chip, *Lab Chip*, 16, 4691–4701 (2016).

Transport of emulsions in heterogeneous environment

Marine LE BLAY^{a,b}, Denis BARTOLO^a

^a*Univ Lyon, Ens de Lyon, Univ Claude Bernard, CNRS, Laboratoire de Physique, F-69342 Lyon, France*

^b*TOTAL SA. Pôle d'Etudes et Recherche de Lacq, BP 47-64170 Lacq, France*

Key words: Fluid mechanics, Capillarity, Depinning physics

We are studying the transport of emulsions through disorder media. Taking advantage of the microfluidic stickers technique, we can produce model emulsions and investigate their transport in heterogeneous environment with controlled geometries. This powerful toolbox allows us to quantitatively address the mobilisation of fluid ganglia in porous media in high content experiments. We combine concepts and tools from fluid mechanics, capillarity and depinning physics to elucidate the intrinsically non-linear response of trapped interfaces in random environments.

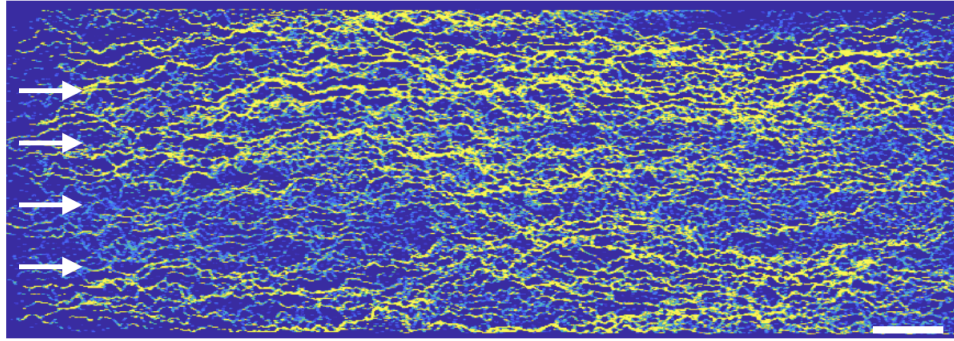


Figure 1: Mean velocity field of a typical experiment, the white arrows indicate the direction of the flow. Scale bar: 1mm.

Adsorption-Induced Slip Inhibition for Polymer Melts on Ideal Substrates

J.D. McGraw^{*a,b,c}, M. Ilton^{d,c}, T. Salez^{e,b,f}, P.D. Fowler^c, M. Rivetti^g, M. Aly^a, M. Benzaquen^{b,h}, E. Raphaël^b, K. Dalnoki-Veress^{c,b}, O. Bäumchen^g

^a*Département de Physique, Ecole Normale Supérieure/PSL Research University, CNRS, 24 Rue Lhomond, 75005 Paris, France*

^b*UMR CNRS Gulliver 7083, ESPCI Paris, PSL Research University, 75005 Paris, France*

^c*Department of Physics & Astronomy, McMaster University, Hamilton, Ontario, Canada, L8S 4M1*

^d*Polymer Science & Engineering Department, University of Massachusetts Amherst, Amherst, MA, 01003, USA*

^e*Univ. Bordeaux, CNRS, LOMA, UMR 5798, F-33405 Talence, France*

^f*Global Station for Soft Matter, Global Institution for Collaborative Research and Education, Hokkaido University, Sapporo, Hokkaido 060-0808, Japan*

^g*Max Planck Institute for Dynamics and Self-Organization (MPIDS), Am Faßberg 17, 37077 Göttingen, Germany*

^h*Ladhyx, UMR CNRS 7646, Ecole Polytechnique, 91128 Palaiseau Cedex, France*

Key words: slip, polymer thin films

1. Abstract

In the study of capillary-driven fluid dynamics [1], relatively simple departures from equilibrium offer the chance to quantitatively model the resulting relaxations. These dynamics in turn provide insight on both practical and fundamental aspects of thin-film and near-surface hydrodynamics. In this talk, we will describe two model experiments—dewetting and capillary levelling—allowing to elucidate polymeric slip in thin polymer films. Slip is a fundamental phenomenon in fluid dynamics that governs liquid transport at small scales. For polymeric liquids, de Gennes predicted [2] that the Navier boundary condition together with the theory of polymer dynamics imply extraordinarily large interfacial slip for entangled polymer melts on ideal surfaces. By comparing two different relatively simple departures from equilibrium, we show [3] that the slip length manifested in a capillary-driven flow experiment in fact depends sensitively on the experimental configuration. A levelling experiment [3, 4] and a dewetting experiment [5] may indeed present vastly different slip boundary conditions even when the probed materials are identical and the surfaces are atomically smooth.

*presenter

References

- [1] Oron *et al.*, Reviews of Modern Physics (1997)
- [2] de Gennes, C.R. Acad. Sci. B (1979)
- [3] Ilton *et al.*, arXiv:1708.03420v2 (2017)
- [4] McGraw *et al.*, Physical Review Letters (2012)
- [5] Bäumchen *et al.*, Physical Review Letters (2009)

Dynamical study of confined bubbles in cylindrical capillary tubes submitted to a Marangoni stress

A. Mansur, B. Reichert, M.-C. Jullien

PSL Research University, ESPCI Paris, Gulliver UMR 7083, 10 rue Vauquelin, F-75005 Paris

Key words: Microfluidics, Marangoni effect, Surfactant dynamics

We study a confined bubble without any surfactants in a cylindrical capillary tube put into motion by a pressure gradient. A surface-tension can be monitored by a linear temperature profile in the capillary. Two classical experimental configurations have been reported: a stress-free bubble pushed by an external phase, known as the Bretherton problem [1], and a bubble set into motion using solely a Marangoni stress [2]. In this study we consider the Bretherton problem including a Marangoni stress, using both a theoretical and an experimental approach. The Marangoni stress that is considered stems from a constant temperature gradient.

On the theoretical side the lubrication equations are written using classical approaches and show that the relative importance of the temperature gradient to the bubble velocity is given by the dimensionless number:

$$\alpha = \frac{3}{2} \frac{\frac{\partial \gamma^*}{\partial x^*}}{(3Ca)^{2/3}} \quad (1)$$

The two regimes given by Bretherton (no temperature gradient) and Mazouchi *et al.* (no external pressure gradient) are recovered.

On the experimental side, we intend to explore the range of parameters for which both contributions are of the same order of magnitude. Our final objective is to understand the role of a Marangoni stress on the droplet dynamics. Care has been taken to build a system surfactant free and with no thermomechanical effect (deformation of the cavity due to a temperature increase). These experiments are currently underway.

References

- [1] Bretherton, F. P. "The motion of long bubbles in tubes." J. Fluid Mech. 10.2 (1961)
- [2] Mazouchi, Ali, and G. M. Homsy. "Thermocapillary migration of long bubbles in cylindrical capillary tubes." Physics of Fluids 12.3 (2000)

Soap films for gas separation

C. Hadji^a, C. Latargez^a, B. Coasne^a, H. Bodiguel^b, B. Dollet^a, E. Lorenceau^a

^aLIPhy, Université Grenoble Alpes and CNRS, F-38402 Grenoble, France

^aLRP UMR5520, Université Grenoble Alpes and CNRS, F-38400 Grenoble, France

Key words: soap film, gas separation, permeability

1. Introduction

Gas and nanoparticle filtration is generally performed via complex and expensive porous membranes facing clogging issues; breaking these current technological limitations relies on decreasing the costs and simplifying the existing protocols. A good alternative lies in specific liquid materials such as soap/foam films, which are thin liquid films stabilized by two amphiphilic surfactant monolayers located at the air/liquid interfaces [1]. The permeability of such films to gas depends on their thickness, the gas solubility in the liquid, and the surfactant monolayers' structure and mutual interactions. Understanding the properties of such systems remains challenging due to their inherent complexity.

2. Our work

The main objective of our study is to understand the phenomenon of gas permeation through a soap film as described in [1]–[3], and how the film properties (thickness, surfactant nature and concentration) affect its performances as a gas filter. We studied the evolution of a system of two gas compartments (air + non soluble C_6F_{14} | air) in a cylindrical syringe, separated by a soap film made of a solution of commercial dish-washing liquid (Fairy©). Only the soluble gas (here, air) will permeate through the membrane to balance both air concentrations (like osmosis phenomena in liquids). We developed a physical model to describe the evolution of the air + C_6F_{14} compartment volume, then compared it to our experimental measurements:

$$V(t) = V_0 [(2\alpha t + 1)^{1/2} - 1] \quad (1)$$

where a (s^{-1}) depends on the unknown film permeability; monitoring the film displacement enables us to compute $V(t)$.

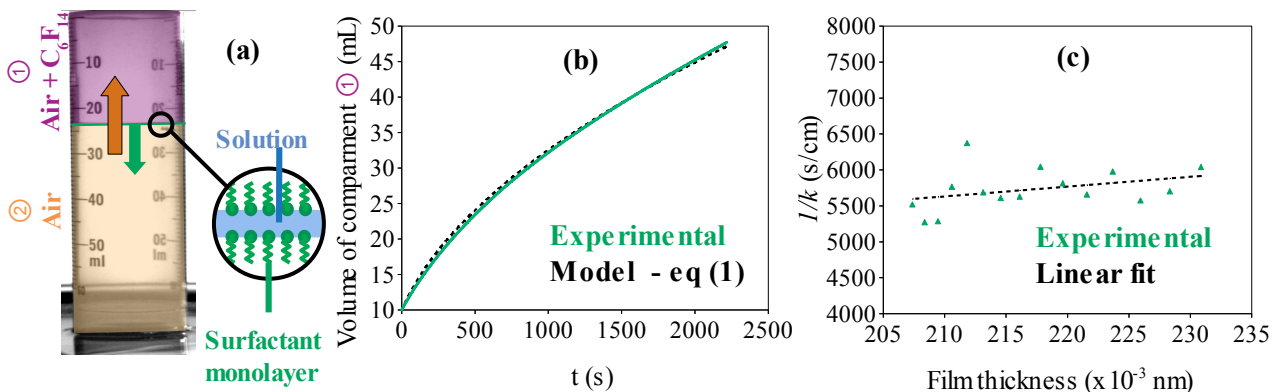


Figure 1: (a) Experimental setup – (b) Evolution of the volume of the upper compartment (air + C_6F_{14}) – (c) Estimated correlation between the film thickness and permeability k .

The permeability values are coherent with similar ones found in other papers [3]–[6]. We were able to estimate the correlation between the film permeability and thickness; this novel result paves the way for a better understanding of foam films. We are currently designing microfluidic equivalents to these systems in order to develop a functioning prototype amenable for repeatable separation of smaller volumes of various gases.

References

- [1] H. M. Princen and S. G. Mason, "The permeability of soap films to gases," *J. Colloid Sci.*, vol. 20, no. 4, pp. 353–375, 1965.
- [2] R. Krustev, D. Platikanov, and M. Nedyalkov, "Permeability of common black foam films to gas. Part 2," *Colloids Surfaces A Physicochem. Eng. Asp.*, vol. 123–124, pp. 383–390, 1997.
- [3] M. Ramanathan, H. –Joachim Müller, H. Möhwald, and R. Krastev, "Foam Films as Thin Liquid Gas Separation Membranes," *ACS Appl. Mater. Interfaces*, vol. 3, no. 3, pp. 633–637, 2011.
- [4] R. Farajzadeh, R. Krastev, and P. L. J. Zitha, "Foam film permeability: Theory and experiment," *Adv. Colloid Interface Sci.*, vol. 137, no. 1, pp. 27–44, 2008.
- [5] L. Saulnier *et al.*, "In situ measurement of the permeability of foam films using quasi-two-dimensional foams," *Colloids Surfaces A Physicochem. Eng. Asp.*, vol. 473, pp. 32–39, 2015.
- [6] R. Krustev, D. Platikanov, A. Stankova, and M. Nedyalkov, "Permeation of Gas Through Newton Black Films At Different Chain Length of The surfactant," *J. Dispers. Sci. Technol.*, vol. 18, no. 6–7, pp. 789–800, 1997.

Fabrication of clamped-clamped microbeams with embedded nanochannels towards nanoparticles sensing

D. Scaiola^{a,b}, S. Stassi^a, P. Renaud^b, C. Ricciardi^a

^a DISAT, Politecnico di Torino, Corso Duca degli Abruzzi 24, Torino 10129, Italy

^b EPFL-STI-INT-LMIS4, École Polytechnique Fédérale de Lausanne (EPFL), Lausanne, Switzerland

Key words: Suspended nanochannel resonator, nanofluidics, nanomechanics, sensor

1. Introduction

Nanoparticles play a big role in nanotechnology field thanks to their widespread applications, from medicine to environment remediation. Moreover, are present also in our «normal life» as in the solar protection, in the toothpaste and in several other products. Because of this spread in use, more and more tools for a precise characterization are required. The actual methods allow for a precise characterization of nanoparticles dimensions and size distribution. However, they also require very expensive instrumentation and time-consuming sample preparation. Suspended micro- and nanochannel resonator (SMR)[1] represent the best approach in terms of costs and easy sample preparation to identify localized masses such as single nanoparticle: in fact, the coupling of a nanofluidic channel with a mechanical resonator offer the possibility to characterize samples directly in liquid with the very high intrinsic resolution of the clamped-clamped beam resonator.

2. Fabrication and characterization

The fabrication process exploited for this kind of devices is very easy and flexible: it allows to produce resonators both with nanoslits (in which the nanometer dimension of the hollow channel is only the height) both with nanochannels (that has both the height and width at the nano-dimension). The process is based on a sacrificial layer approach: a 50 nm thick silicon layer is first deposited and structured by dry-etching techniques and then it is removed using the Xenon Difluoride to create a hollow channel buried in the silicon dioxide. The choice to use only dry process in due to avoid as much as possible problem of stiction during the releasing steps.

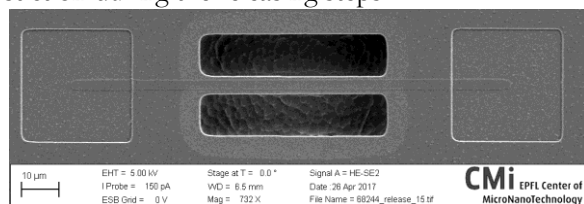


Figure 1: Microbeam with nanoslit channel (length 80 μm, width 5 μm, height 50 nm)

After the fabrication part, preliminary characterizations of the mechanical proprieties of the clamped-clamped beam and fluidics one of the nanochannel have been already done giving promising results on the achievable sensitivity of the resonating sensor: between 200-300 ag/Hz with the nanoslit devices and around 20 ag/Hz with the nanochannel based ones.

References

[1] Burg, Thomas P., and Scott R. Manalis. "Suspended microchannel resonators for biomolecular detection." *Applied Physics Letters* 83.13 (2003): 2698-2700.

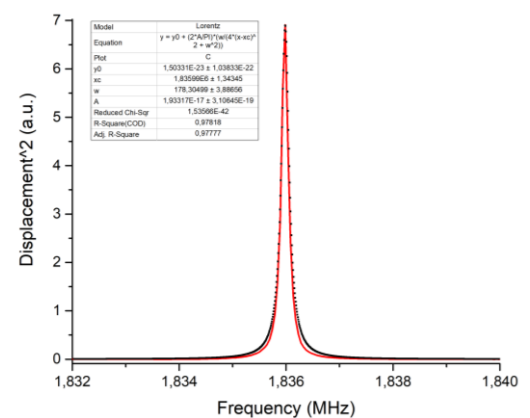


Figure 2: Mechanical Characterization in vacuum: the Lorentzian fit of the first mode peak. A Q factor of about 10.000 has been measured.

Liquid phase exfoliation of graphene in hydrocavitating labs-on-a-chip

X. Qiu^a, V. Bouchiat^b, D. Colombet^a, F. Ayela^a

^aLEGI, Univ. Grenoble Alpes, 38000 Grenoble, France

^bInstitut Néel, Univ. Grenoble Alpes, 38000 Grenoble, France

Key words: Graphene, hydrodynamic cavitation, lab-on-a-chip

Abstract

Graphene, a single layer of graphite, has attracted a great deal of interest due to its extraordinary properties in mechanical and electronic domains. However, massive production of few layers graphene has so far been very limited. Nowadays, liquid phase exfoliation is considered as one of the most promising process for production of multi-sheets on a large scale. Acoustic cavitation has been widely used by researchers because of its simplicity of implement, but ultrasound leads to damage in the graphene structures. Hydrodynamic cavitation and single liquid phase have been reported to exfoliate graphite as well. However, input pressure should increase up to 200 bar. Indeed, bubbles collapse and flow shear rate have both been proposed as possible exfoliation mechanisms. From a fundamental and application point of view, it would be interesting to know which force could lead a more effective exfoliation. These questions reach to the core of our research project devoted to the liquid phase exfoliation of graphene in labs-on-a-chip. In our application, lab-on-a-chip is a silicon Pyrex microfluidic device that integrates a localized micro step giving way to a gap of height $\approx 130 \mu m$. The main advantage provided by this system lies in the wide range of the flow regimes that can be studied with a given set of reactors, such as laminar or turbulent single liquid phase flow, and cavitating two phase flow, with a pressure drop below 10 bars[1]. Fig.(1) shows an outline of graphene exfoliation by lab-on-a-chip. Up

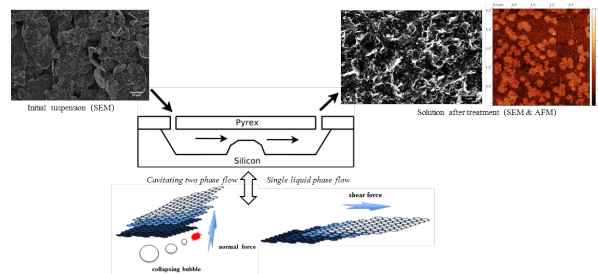


Figure 1: Liquid phase exfoliation of graphene in lab-on-a-chip

to now, we have studied microflows in which exfoliation is the consequence of the high shear rate of the flow and of the collapse of bubbles. The solution was initially a graphite powder suspension with a solid concentration of 50 g/L. The aqueous suspension is stabilized by a surfactant. It was processed during 2016 cycles, under a pressure drop of 10 bar and with a flow rate of 16 liters per hour. The effective time during which each microparticle has been submitted to high shear rate and cavitation is around 6 seconds. Recent results have demonstrated that such hydrodynamic cavitation on a chip could exfoliate the graphite suspension in a homogenous way. Monolayers and multilayers of graphene have been obtained after the cavitation treatment. The production of monolayers and multilayers of graphene with a high yield and a low cost is promising for many applications.

References

- [1] X Qiu, W Cherief, D Colombet and F Ayela , A simple process to achieve microchannels geometries able to produce hydrodynamic cavitation, Journal of Micromechanics and Microengineering, 27, 047001 4 (2017)

Transport of nano-objects in narrow channels: influence of Brownian diffusion, confinement and particle nature

O. Liot^{a,b,c}, M. Socol^a, L. Garcia^a, J. Thiéry^a, A. Figarol^{d,e}, A.-F. Mingotaud^d, P. Joseph^a

^aLAAS-CNRS, Université de Toulouse, CNRS, Toulouse, France

^bFédération FERMaT, INP Toulouse

^cPresent address: Institut Lumière Matière, 10 rue Ada Byron, 69100 Villeurbanne, France

^dLaboratoire des IMRCP, UMR CNRS 5623, Université de Toulouse, 31062, Toulouse, France

^ePresent address: Institut de Pharmacologie et de Biologie Structurale, CNRS, Université de Toulouse, F-31077 Toulouse, France

Key words: Colloidal transport, Brownian diffusion, soft particles, polymersomes

Transport of confined colloids in nanochannels is a key for many situations in biology (blood flow, flow cytometry, DNA analysis [9]), and flows in porous media [1] (chemical engineering with polymer processing, clogging [15, 4], separation [14], geophysics i.e. fractured rocks [16]). If the behaviour of advected particles or colloids in microchannels begins to be well understood both theoretically [12] and experimentally [11, 10], this field remains very active. Effect of wall roughness is also very important in natural systems [2, 8]. Furthermore transport of vesicles and soft particles in microfluidic devices is an emerging topic with dramatic implications such as drug vectorization [6] or in the comprehension of the transport of biological objects. Behaviour of soft capsules or vesicles under flow is quite well understood [5, 13]. Nevertheless, the cross effects of Brownian diffusion, particle nature and confinement are still not clear. Yet, in the case of sub-micrometric particles, these effects are crucial to explain transport in porous media. Moreover, the entrance geometry can have substantial effects on particle distribution in the channels and so on their transport in a pore [11].

We study experimentally the transport of solid and capsule-like objects in nanoslits. Solid particles are carboxylate-modified polystyrene beads whereas soft objects are polymer auto-assemblies called polymersomes [3]. Channels are etched in silicon with different etching depths between 330 and 3390 nm and covered with glass. The flow is pressure-driven and particles are tracked using fluorescence microscopy. We have access to large statistics. We estimate the expected velocity taking into account Faxén's law and hydrodynamic interactions [7].

Results let appear two regimes for solid beads. In the first one the experimental mean velocity is similar to the theoretical one whereas in the second one the mean velocity of the objects is lower of about 20%. This can be related to cross effects of confinement and Brownian diffusion. The second regime appears at the lower confinement and the lower Brownian diffusion. The transition can be observed in some cases by varying the advection in the pore. The physical mechanism of this regime distinction has for origin the homogeneity or not of the particle distribution in the channels depth, due to the pore entrance geometry. This is demonstrated by deriving the position distributions from the velocity ones.

Concerning the polymersomes, the second regime seems to disappear. Only the transition is visible for similar particles diameter and confinement. This could be due to interactions between mechanical softness of these objects and the flow at the entrance of the channels.

References

- [1] Bradford, S. A. & Torkzaban, S. Colloid Transport and Retention in Unsaturated Porous Media: A Review of Interface-, Collector-, and Pore-Scale Processes and Models. *Vadose Zone Journal*, 7(2), 667 (2008).
- [2] Charru, F., Larrieu, E., Dupont, J.-B., & Zenit, R. Motion of a particle near a rough wall in a viscous shear flow. *Journal of Fluid Mechanics*, 570, 431 (2007).
- [3] Dionzou, M., Mor{\e}re, A., Roux, C., Lonetti, B., Marty, J.-D., Mingotaud, C., Joseph, P., Goudoun{\e}che, D., Payr{\e}, B., L{\e}onetti, M., & Mingotaud, A.-F. Comparison of methods for the fabrication and the characterization of polymer self-assemblies: what are the important parameters? *Soft Matter*, 12(7), 2166–2176 (2016).
- [4] Dressaire, E. & Sauret, A. Clogging of microfluidic systems. *Soft Matter*, 13(1), 37–48 (2017).

- [5] Lefebvre, Y. & Barth{\e}s-Biesel, D. Motion of a capsule in a cylindrical tube: effect of membrane pre-stress. *Journal of Fluid Mechanics*, 589, 157–181 (2007).
- [6] Maeda, H. Macromolecular therapeutics in cancer treatment: the EPR effect and beyond. *Journal of Controlled Release: Official Journal of the Controlled Release Society*, 164(2), 138–144 (2012).
- [7] Pasol, L., Martin, M., Ekiel-Jezewska, M., Wajnryb, E., Blawdziewicz, J., & Feuillebois, F. Motion of a sphere parallel to plane walls in a Poiseuille flow. Application to field-flow fractionation and hydrodynamic chromatography. *Chemical Engineering Science*, 66(18), 4078–4089 (2011).
- [8] Ranchon, H., Cacheux, J., Reig, B., Liot, O., Terrapanich, P., Leichl{\e}, T., Joseph, P., & Bancaud, A. Accelerated transport of particles in confined channels with high roughness amplitude. *Langmuir* (2018).
- [9] Ranchon, H., Malbec, R., Picot, V., Boutonnet, A., Terrapanich, P., Joseph, P., Leichl{\e}, T., & Bancaud, A. DNA separation and enrichment using electro-hydrodynamic bidirectional flows in viscoelastic liquids. *Lab on a Chip*, 16(7), 1243–1253 (2016).
- [10] Ranchon, H., Picot, V., & Bancaud, A. Metrology of confined flows using wide field nanoparticle velocimetry. *Scientific Reports*, 5(1) (2015).
- [11] Staben, M. E. & Davis, R. H. Particle transport in Poiseuille flow in narrow channels. *International Journal of Multiphase Flow*, 31(5), 529–547 (2005).
- [12] Staben, M. E., Zinchenko, A. Z., & Davis, R. H. Motion of a particle between two parallel plane walls in low-Reynolds-number Poiseuille flow. *Physics of Fluids*, 15(6), 1711 (2003).
- [13] Vlahovska, P. M., Podgorski, T., & Misbah, C. Vesicles and red blood cells in flow: From individual dynamics to rheology. *Comptes Rendus Physique*, 10(8), 775–789 (2009).
- [14] Wu, Z. & Hjort, K. Microfluidic Hydrodynamic Cell Separation: A Review. *Micro and Nanosystems*, 1(3), 181–192 (2009).
- [15] Wyss, H. M., Blair, D. L., Morris, J. F., Stone, H. A., & Weitz, D. A. Mechanism for clogging of microchannels. *Physical Review E*, 74(6) (2006).
- [16] Zhang, W., Tang, X., Weisbrod, N., & Guan, Z. A review of colloid transport in fractured rocks. *Journal of Mountain Science*, 9(6), 770–787 (2012).

Ultrasound transmission through microfluidics-generated liquid foams

L. Champougny^a, J. Pierre^b, V. Leroy^c and M.-C. Jullien^a

^a*Gulliver, CNRS, ESPCI Paris, PSL Research University, 10 rue Vauquelin, Paris, France*

^b*Institut d'Alembert, Université Pierre et Marie Curie, CNRS, Paris, France*

^c*Laboratoire Matière et Systèmes Complexes, Université Paris-Diderot, CNRS, Paris, France*

Key words: acoustofluidics, ultrasound, liquid foams, monodisperse bubbles

While the acoustic properties of solid foams, which are frequently used for soundproofing purposes, have been abundantly characterized [1], sound propagation in liquid foams remains poorly understood. J. Pierre and collaborators have recently investigated the transmission of ultrasound through polydisperse liquid foam samples [2, 3]. Their study showed that the mechanical coupling between the liquid network in the foam and the thin liquid films separating the bubbles could result in a large attenuation, associated to a resonant behavior [4].

The acoustic propagation in a foam strongly depends on its structural parameters (number, surface and thickness of the films, liquid fraction, among others), all of which were not well characterized in previous experiments. Further progress thus requires to investigate the acoustic response of well-controlled foam structures. We introduce a new experimental setup designed to study the transmission of ultrasound (frequencies in the range 70 – 1000 kHz) through model monodisperse liquid foam samples generated by microfluidics. We will present measurements of the acoustic transmission through monodisperse bubble monolayers of various liquid fractions and bubble sizes. The analysis of these measurements will allow us to retrieve the sound velocity and attenuation in bubble monolayers as functions of their structural parameters.

Additionally, preliminary results on bubble bilayers already show a qualitative difference between the transmission through bubble monolayers and bilayers. This is likely a signature of the free liquid films separating the top and bottom bubbles in the bilayer. This discrete approach, allowing to isolate the signature of a single layer of free films in the acoustic response, will contribute to a better understanding of the dissipation in liquid foams. On the long term, this work could contribute to the design of optimized acoustic metamaterials created by solidification of liquid foams.

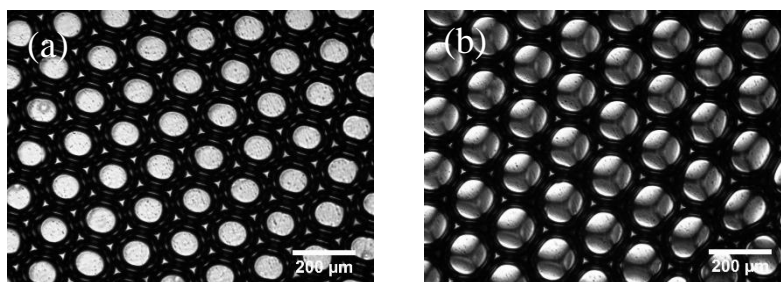


Figure 1: Model foams generated by microfluidics. (a) Monodisperse bubble monolayer – (b) Monodisperse bubble bilayer.

References

- [1] Attenborough, Acoustical characteristics of porous materials. *Physics Reports* 82(3), pp. 179-227, 1982.
- [2] Pierre, Elias & Leroy, *Ultrasonics*, Volume 53, pp. 622-629, 2013.
- [3] Pierre *et al.* *Physical Review E*, Volume 91, 2015.
- [4] Pierre, Dollet & Leroy, *Physical Review Letters*, 112(14), 2014.

Using Microfluidic as a Tool for Biological Macromolecular Serial Crystallography on a Synchrotron Beamline : Proxima-1

Chaussavoine Igor, Montaville Pierre, Gourhant Patrick, Mateo Tiphaine, Chavas Leonard.
Synchrotron SOLEIL, L'Orme des Merisier, Saint-Aubin, 91192 Gif-sur-Yvette, France

Key words: Crystallography, Synchrotron, Microfluidic

Abstract

Example of bibliographic citations : [1],[2],[3]

One of the major evolution in recent macromolecular crystallography experiments lies in the implementation of serial crystallography, originally developed for hard x-ray Free-Electron Lasers (FELs), and later adapted to synchrotron sources. These new approaches, allow to further expand the spectre and possibilities in crystallography. The techniques validated to date bring successful results, yet suffer from the requirement of extensive amounts of sample crystals and recorded images to start structure analysis; potentially, this also requires long beamtime shifts at x-ray FELs. At various synchrotron sources including SOLEIL, serial crystallography was adapted by using microfluidic chips¹ to handle batches of macromolecular crystals and expose those to the synchrotron beam. These new developments allow acquiring diffraction data over several degrees *per* crystal, permitting to drop consequently the number of crystals required for acquiring a complete data set. In addition of facilitating a better control during serial crystallography experiments, microfluidic chips provide with the possibility of mastering the crystal environment, the injection of ligands, or even opens access to diffraction experiments on biologically hazardous molecules. Moreover, the trapping method employed within the microfluidic chips facilitates bypassing most of the chemical issues currently occurring when handling and preparing macromolecular crystals for diffraction experiments.

The presentation will highlight the results of microfluidic induced macromolecular serial crystallography at synchrotron SOLEIL. Using specific patterns inspired from an experiment by Lyubimov², macromolecular crystals or macromolecular crystal containing cells are trapped at known and precise positions within a microfluidic chip. The chip can then be handled and oriented using an adapted 3D-printed frame placed on the goniometer at PROXIMA-1³ beamline. Our initial results illustrated here were obtained using an *in house* device; complete data could be acquired with high redundancy prior to solving the structure of a reference protein sample.

References

1. Igor Chaussavoine. Realisation of microfluidic chips for macromolecular X-ray crystallography. M2 report Paris saclay, 2017
2. Artem Y. Lyubimov. Capture and x-ray diffraction studies of protein microcrystals in a microfluidic trap array. Biological crystallography, 2015.
3. P. Gourhant P. Legrand O. Roudenko L. Roussier I. Ascone, E. Girard and A. W. Thompson. Proxima 1, a new beamline on the third generation sr source soleil combining px and single-crystal bioxas. http://www.slac.stanford.edu/econf/C060709/papers/259_THPO43.PDF.

Self-cleaning slippery infused surfaces for dairy processing

S. Zouaghi^a, T. Six^a, S. Bellayer^a, S. Moradi^b, S.G. Hatzikiriakos^b, T. Dargent^c, V. Thomy^c, Y. Coffinier^c, C. Andre^{a,d}, G. Delaplace^a, M. Jimenez^a

^a UMET, CNRS-UMR 8207, Villeneuve d'Ascq, France

^b University of British Columbia, Faculty of Applied Science, Chemical and Biological Engineering, Vancouver, Canada

^c IEMN, CNRS-UMR 8520, Villeneuve d'Ascq, France

^d Hautes Etudes d'Ingénieur (HEI), Lille, France

Key words: SLIPS, self-cleaning, Dairy processing

1. Introduction

In dairy pasteurization processes, biofouling is a major issue. Indeed, in order to avoid microbial contaminations, milk needs to be heated to specific temperatures (72-85°C), which generates mineral and proteinaceous deposits on stainless steel walls. This heat-induced fouling impairs the good execution of the process through the addition of an increasing thermal resistance to the system and is therefore a threat to food safety. Moreover, the required cleaning procedures burden both the financial balance and the environmental footprint of thermal processes.

As for others applications where biofouling is a key parameter, a biomimetic approach, from Lotus leaves to Nepenthes pitcher plants, has been considered. In the first case, the dual-scale roughness (i.e. a micrometric roughness supporting a nanometric roughness) of its surface allows them to reach the metastable Cassie-Baxter wetting state, in which air remains trapped between the liquid and the solid surface, which results in very high contact angles and very low contact angle hysteresis. For the second one, the impregnation of the rough surface by a non-miscible low surface energy liquid leads to a stable state with a quasi-null hysteresis even for liquid presenting a low surface energy [1].

2. Results

In this work, different stainless steel based surfaces have been texturized *via* femtosecond laser ablation to generate dual-scale cauliflower-like structures on its surface [2] and were then modified either by (i) silanization with Perfluorodecyltrichlorosilane or (ii) silanization followed by impregnation with a fluorinated oil to create Slippery Liquid Infused Porous Surfaces (SLIPS-like). All surfaces were tested for their fouling properties in a pilot pasteurization equipment allowing to mimic the conditions of an industrial pasteurization process (heating between 65 to 85°C, model milk flow rate equal to 300L/h during 1.5h) [3]. Among the different results obtained, we will present outstanding ones regarding antifouling properties of dual-scaled roughness surfaces in dairy processing conditions, with a reduction of fouling by more than 90% in weight [4].

References

- [1] V. Senez, V. Thomy, R. Dufour, Nanotechnologies for synthetic super non-wetting surfaces, ISBN 978-1-84821-579-5, Wiley-ISTE, 177 pages (2014).
- [2] A.-M. Kietzig, S. G. Hatzikiriakos, and P. Englezos, attened Superhydrophobic Metallic Surfaces Langmuir, vol. 25, no. 8, pp. 4821–4827 (2009).
- [3] M. Jimenez, G. Delaplace, N. Nuns, S. Bellayer, D. Deresmes, G. Ronse, G. Alogaili, M. Collinet-Fressancourt, and M. Traisnel, oward the understanding of the interfacial dairy fouling deposition and growth mechanisms at a stainless steel surface: A multiscale approach, J. Colloid an interface Sci., vol. 404, pp. 192–200 (2013).
- [4] Zouaghi S., Six T., Bellayer S., Moradi S., Hatzikiriakos S.G., Dargent T., Thomy V., Coffinier Y., Andre C., Delaplace G., Jimenez M., Antifouling biomimetic liquid-infused stainless steel: application to dairy industrial processing, ACS Appl. Mater. Interfaces 9, 31, 26565-26573 (2017)

Laboratoire sur puce pour la détection d'événements cellulaires rares

M. Valette ^{ab}, R. Courson ^{ab}, C. Blatché ^{ab}, A. M. Gué ^{ab}

^aL'AAS-CNRS, University of Toulouse, 7 Avenue du Colonel Roche, BP 54200, 31 031 Toulouse cedex 4, France

^bUniv de Toulouse, L'AAS, F-31400 Toulouse, France

Mots clés: cellules souches adipeuses, ASCs, déformabilité, filtration hydrodynamique, tri immunologique

1. Introduction

L'objectif du projet est de développer un système d'analyse miniaturisé permettant d'isoler spécifiquement des espèces cellulaires présentes en très faible proportion dans les milieux liquides. Les cellules d'intérêt sont les cellules souches adipeuses (ASCs), cellules souches multipotentes qui ont la capacité de se différencier en de nombreuses cellules telles que les chondrocytes, les adipocytes et les ostéoblastes. Ces cellules se trouvent en grande majorité dans le tissu adipeux mais peuvent également être retrouvées dans le sang (elles sont alors dites circulantes). La séparation de ces cellules du milieu sanguin ouvrirait de nombreuses perspectives dans le diagnostic précoce du diabète de type II ou en médecine régénérative.

2. Approche retenue pour un LOC de séparation des ASCs en milieu sanguin

La taille des cellules cibles est un critère essentiel pour le choix des techniques de tri à employer. Des caractérisations effectuées par FACS (Fluorescent Activated Cell Sorting) calibré avec des billes de diamètres 5, 10, 15 et 20 μm (figure 1) montrent que les ASCs ont un diamètre supérieur à 10 μm , avec une grande variété de tailles et ne se distinguent donc pas des leucocytes hors lymphocytes.

Par ailleurs les antigènes CD45 et CD31 exprimés par les leucocytes sont discriminants puisqu'ils ne sont pas exprimés par les ASCs.

Compte-tenu de ces caractéristiques, nous avons donc décidé de développer un dispositif comportant 2 étapes de tri complémentaires et successives. La première étape consiste à éliminer les éléments dont le diamètre est inférieur ou égal à 10 μm , dont en particulier les globules rouges. Pour ce faire, nous utilisons un principe de filtration hydrodynamique.

La seconde étape aura pour but d'éliminer toutes les cellules hématopoïétiques par exclusion des cellules exprimant l'antigène CD45 et/ou CD31. Cette étape sera réalisée en utilisant une technique de type « cell rolling ».

3. Premiers résultats

Une première génération de puces de séparation hydrodynamique a été réalisée. Elle montre bien la séparation des particules autour du rayon critique choisi mais avec une efficacité insuffisante. La caractérisation des écoulements à l'aide de particules fluorescentes submicrométriques montre des effets de recirculation pénalisants à l'intersection des canalisations de filtration. Une étude par simulation numérique a permis de modifier le design des puces afin d'éliminer ces effets. Les dispositifs sont en cours de test.

La première étape pour la mise en œuvre du principe de séparation par « cell rolling » est la mise au point d'une technologie de greffage localisée d'anticorps CD45. La méthode retenue utilise le dépôt d'une première couche de SAMs (11-mercaptopundecanoïque (MUA) et 6-mercaptophexanol (MH)) sur laquelle les anticorps sont greffés. Ces travaux sont en cours.

Indépendamment, nous avons choisi d'évaluer les propriétés de déformabilités des ASCs afin de savoir si ce critère était discriminant et pouvait être utilisé pour la séparation des ASCs. Un dispositif microfluidique a été développé permettant de piéger une cellule (unique) dans un réservoir et d'appliquer différentes pressions afin d'en déterminer le module d'Young et/ou la tension corticale. Le dispositif a été testé sur des cellules souches adipeuses mises en culture. Les expériences mettent en évidence la déformation marquée des cellules. Les résultats sont en cours d'exploitation.

Bottom-up assembly of cells in flow with dielectrophoresis

Jonathan Cottet^{a,b}, Olivier Fabregue^a, Julien Marchalot^a, Riccardo Scorretti^a, François Buret^a,
Marie Frénéa-Robin^a and Philippe Renaud^b

^aUniv. Lyon, ECL, UCB Lyon 1, CNRS, AMPERE, F-69130, Lyon, France

^bÉcole Polytechnique Fédérale de Lausanne, EPFL-STI-IMT-LMIS4, Station 17, CH-1015 Lausanne, Suisse

Key words: Cell trapping, Dielectrophoresis, Microfluidics, Bottom-up assembly

Electrochemotherapy (ECT) consists in using electric fields to enhance the delivery of chemotherapeutic agents directly into cancer cells. However, the full development of this therapeutic approach requires a proper understanding of electric field impact on biological tissues. While in vitro studies performed on isolated cells provide useful information on how field pulses induce biological membrane permeabilization, more realistic 3D in vitro models are required to mimic the behavior of cells in a tumor or a tissue. Multicellular constructs can be used as simple models of tumor microregions for optimization of electropulsation protocols.

We present a microfluidic platform allowing dielectrophoresis-assisted formation of cell aggregates of controlled size and composition under flow. When specific experimental conditions are met (medium composition, electric field intensity and frequency), negative dielectrophoresis (nDEP) allows efficient concentration of cells towards electric field minima and subsequent aggregation. This bottom-up assembly strategy offers several advantages with respect to the targeted application: first, DEP offers precise control of cell spatial organization, which can be adjusted by optimizing electrode design. Then, rapid establishment of cell-cell interactions is allowed thanks to dipole-dipole attraction forces between neighboring cells.

The trapping geometry of our chip is composed of 8 electrodes disposed in a circle. Several parameters have been tested in simulations to find the best configurations for trapping in flow. Those configurations have been tested experimentally with both polystyrene beads and HEK cells. Figure 1 illustrates the trapping of HEK cells under flow to create a small aggregate using 3 electrodes.

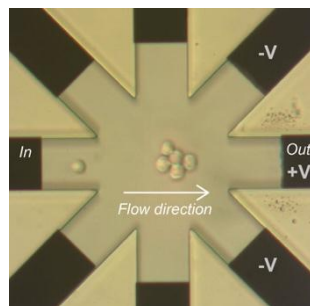


Figure 1: Trapping of HEK cells under flow.

This study demonstrates the potential of using planar electrodes and dielectrophoresis to create cell aggregates under flow. The created aggregates can be further studied with impedance spectroscopy or electrorotation and electroporated using other electrodes. Both homogeneous and composite aggregates can be generated using this approach.

Invited conference (II)

The Physics and Engineering of Active Matter

R. Di Leonardo^a

^aDipartimento di Fisica, Sapienza Università di Roma, Roma I-00185, Italy

Key words: Active matter, microfabrication, flagellar motility

1. Abstract

Dense suspensions of swimming bacteria display striking motions that look extremely vivid when compared to the thermal agitation of colloidal particles of comparable size. These suspensions belong to a wider class of non-equilibrium systems that are now collectively referred to as active matter [1]. Research in active matter physics deals with the fundamental aspects underlying some distinctive properties of these systems, such as the emergence of collective behavior and rectification phenomena. From a more engineering perspective, however, active matter can be looked at as a special kind of fuel: a small droplet of an active fluid can be used to propel micro-machines inside miniaturized chips, with no need of external driving fields or control. Using advanced tools for 3D optical imaging, manipulation and fabrication we study complex phenomena in active matter with direct and quantitative methods. I will review our recent work in this direction, from off-equilibrium transport and stationary states in active matter [2] to the use of genetically engineered bacteria as controllable propellers for synthetic micro-machines (Fig. 1) [3].

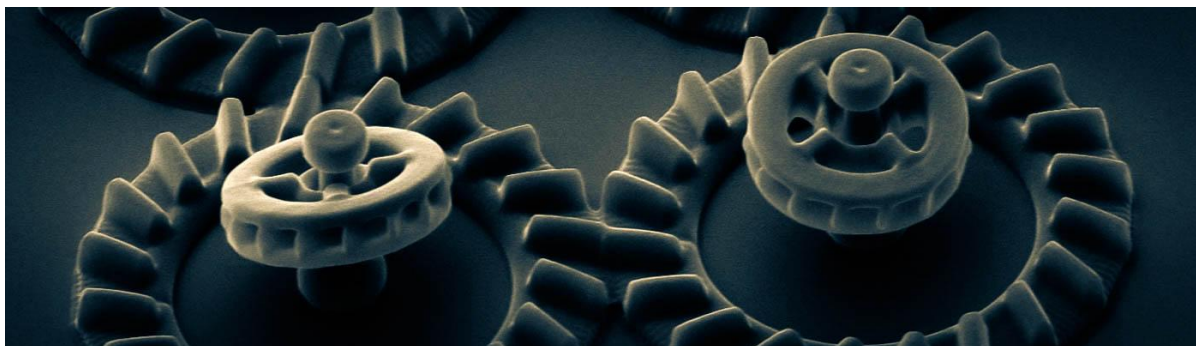


Figure 1: SEM image of rotary micromotors driven by bacteria.

References

- [1] C. Bechinger et al. Active particles in complex and crowded environments, *Rev. Mod. Phys.*, 88, 045006, (2016).
- [2] N. Koumakis et al. Targeted delivery of colloids by swimming bacteria, *Nature Communications*, 4, 2588, (2013).
- [3] G. Vizsnyiczai et al. Light controlled 3d micromotors powered by bacteria, *Nature Communications*, 8, 15974, (2017).

Drops, bubbles, etc ... (II)

Dynamics of fibers transported in confined viscous flow

J. Cappelletto^a, C. Duprat^b, O. du Roure^a, A. Lindner^a

^a*Physique et Mécanique des Milieux Hétérogènes, CNRS UMR 7636, ESPCI Paris, Université Paris Diderot, Paris, France*

^b*LadHyX, CNRS UMR 7646, Ecole Polytechnique, Université Paris-Saclay, Palaiseau, France*

Key words: Fibers, flexible, confinement, microfluidic, bending and buckling

The transport and dynamics of elongated objects has been extensively studied in unbounded media such as the situation of sedimenting fibers in Stokes flow. Here we focus our study on the dynamics of fibers transported in pressure-driven flows in confined geometries. We show that the confinement tunes the friction forces on the fiber and as a consequence the velocity of the object becomes anisotropic for high confinement [1]. These passive hydrodynamic effects lead for example to a lateral drift of simple straight fibers transported in confined channels. Elastic fibers on the other hand can be deformed while transported. Fibers perpendicular to the flow will bend while parallel fiber can show a buckling instability.

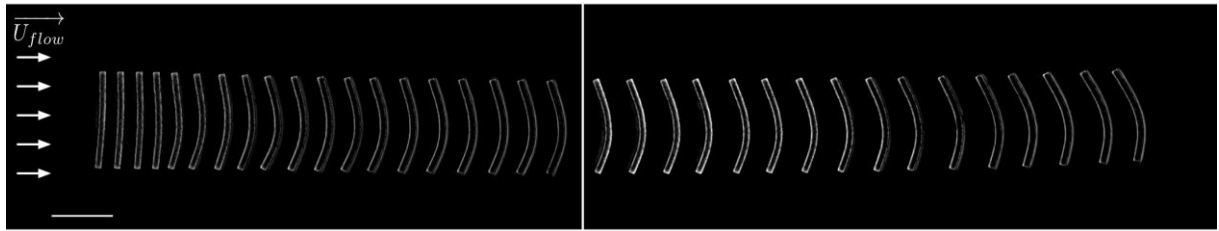


Figure 1: Bending of a confined flexible fiber transported in a confined viscous external flow.

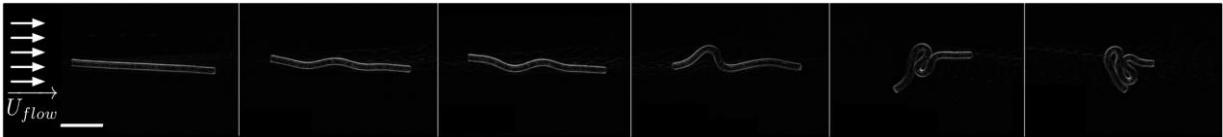


Figure 2: Buckling of confined flexible fibers transported in a confined viscous flow.

We chose to investigate these effects with a combination of well-controlled microfluidics experiments and simulations using modified Brinkmann equations [2]. We control shape, orientation, and mechanical properties of our particles using micro-fabrication techniques [3] and in-situ characterization methods [4].

We show that the bending of the perpendicular fiber is proportional to an elasto-viscous number and we fully characterize the influence of the confinement on the deformation of the fiber. Experiments on parallel flexible fibers reveal the existence of a buckling threshold.

References

- [1] H. Berthet et al., Phys. Fluids, 25, 103601 (2013)
- [2] M. Nagel et al., Journal of Fluid Mechanics, (2017)
- [3] D. Dendukuri et al., Macromolecule, 41 (22), 8547-8556, (2008)
- [4] C. Duprat et al., Lab on a Chip, 15, 244 (2015)

Deformability-based (micro)fluidic sorting

Doriane VESPERINI^a, Anne-Virginie Salsac^a, Anne Le Goff^a

^a Sorbonne Universités, Université de technologie de Compiègne, UMR CNRS 7338 BMBI

Key words: capsule, sorting, deformation

1. Introduction

Biomedical applications often require to sort cells according to their intrinsic properties. Cell deformability has been identified as a promising biomarker in several pathologies. As microfluidic systems allow to generate well-controlled hydrodynamic forces and to manipulate microscopic objects individually, they are good candidates for probing cell deformability. A simple sorter, consisting of a straight channel obstructed by an obstacle and connected to a diverging chamber, has been studied numerically and suggested as a way to separate microcapsules according to their mechanical properties [1]. In such a system, the trajectory of capsules depends on their deformability but also on their lateral position in the main channel [2].

2. Methods

Channels are fabricated in PDMS. A flow focusing module is placed upstream of the main channel in order to center the capsules. The main channel is obstructed by a semi-cylindrical obstacle and suddenly widens. The flow in the diverging chamber is split towards five different exits. Channel dimensions are adapted to the size of objects to be sorted.

Ovalbumin microcapsules are diluted in glycerol and infused into the chip by the means of a pressure controller. Non-adherent cell lines are cultured in liquid media and treated with drugs (blebbistatin or cytochalasin D) to modify their mechanical properties.

3. Results

We first perform experiments at low pressures, so that hydrodynamic forces induce no significant deformation of the capsules. In this regime, capsule populations can be sorted according to their size. We measure how the trajectory of micro-objects in the sorter is influenced by their off-centering. Using a flow focusing module, we show that we can keep the off-centering below a desired threshold. We then demonstrate that a population of homogeneous size can be sorted according to deformability, provided objects are well-centered. Using microcapsules with controlled mechanical properties we show that our system can separate micro-objects whose surface shear modulus differs only by a factor 3.

References

- [1] L. Zhu et al. A microfluidic device to sort capsules by deformability: a numerical study. *Soft Matter*, 10, 7705-7711 (2014)
- [2] E. Häner, PhD thesis, University of Manchester (2017)
- [3] D. Vesperini et al., Deformability- and size-based microcapsule sorting, *Medical engineering and Physics*, 48 68-74(2017)

Nanofluidic

Direct measurement of liquid flow rate up to picoliter per minute

P. Sharma^a, J. F. Motte^b, F. Fournel^c, E. Charlaix^a, C. Picard^a

^aUniv. Grenoble Alpes, CNRS, LIPhy, 38000 Grenoble, France

^bUniv. Grenoble Alpes, CNRS, Grenoble INP, Institut Néel, 38000 Grenoble, France

^cCEA, LETI, MINATEC, 38054 Grenoble, France

Key words: flow rate sensor, nanopore, diffusio-electro-osmosis, blue energy

The maturation of nanofluidics over the last two decades has benefited from significant instrumental development in order to measure physical quantities associated to flow and transport at the nanoscale. The measurement of electrical current, for instance, through a single nanochannel, such as an ion channel within a lipid bilayer can now be done with commercial apparatus. These developments contributed to the understanding of transport phenomena in nanopores related to various applications ranging from DNA sequencing to oil extraction and purification, but also water desalination and reversely electricity production by means of electro-diffusio-osmosis phenomena based on ion selective transport in nanopores.

In this framework, a central quantity that remains challenging to measure at the scale of an individual nanopore, is flow rate. The best commercial flow rate sensor gives the ability to measure flow rates of the order of 10 nL/min that remain three decades larger than those typically expected with water in a single nanopore of 100 nm diameter. A few approaches exist though to probe such small flow rates but indirectly and in specific configurations only[1].

To overcome these limitations we developed a simple versatile approach that allows one to perform direct liquid flow rate measurements with a detection threshold of the order of 1 pL.min⁻¹ [2]. This approach, that is the subject of a patent that will be submitted in the coming days, is applicable to any type of liquid and is not limited to the study of a specific nanofluidic system. This communication aims at describing the principle of the measurement method and the building of a demonstrative sensor based on this approach. The capabilities of the sensor are illustrated with the characterization of pressure driven flow through cylindrical micro-capillaries used as benchmark systems that can be easily calibrated. This demonstrative sensor is shown to cover three decades of flow rates ranging from 1 pL/min to 1 nL/min. The measure of flow rate through a single conical nanopore within a 1 micron thick silica membrane will be considered as a last example that opens new possibilities for the study of electro-osmosis in strong confinement.



Figure 1: Measured flow rate through calibrated capillaries (left), SEM picture of a nanopore (center) and theoretical velocity field in low Reynolds regime (right).

References

- [1] Eleonora Secchi, Sophie Marbach, Antoine Nigués, Derek Stein, Alessandro Siria, and Lydéric Bocquet, *Nature*, 537(7619), 210-213, 2016
- [2] Preeti Sharma. *Coupled electro-diffusio-osmosis fluxes in a single nanochannel for energy conversion*, PhD thesis. Université Grenoble Alpes, 2017.

Active Sieving : from flapping nano-doors to vibrating nanotubes

S. Marbach^a, A. Niguès^a, A. Siria^a, D. Dean^b, L. Bocquet^{ac}

^a*laboratoire de physique statistique, Ecole Normale Supérieure, 75005 Paris, France*

^b*laboratoire onde et matière d'aquitaine, Université de Bordeaux, 33400 Talence, France*

^c*Institut Pierre-Gilles de Gennes, 75005 Paris, France*

Key words: out of equilibrium sieving, filtration, Maxwell demon

1. Abstract

Filtering specific molecules is a challenge faced for several vital needs: from biomedical applications like dialysis to the intensive production of clean water. The domain has been boosted over the last decades by the possibilities offered by nanoscale materials [1]. Filtration is however always designed according to a passive sieving perspective: a membrane with small and properly decorated pores allows for the selection of the targeted molecules. This inevitably impedes the flux and transport, making separation processes costly in terms of energy.

Here we investigate alternative approaches to separation and filtration. We explore the possibility of non-equilibrium sieving, harnessing the difference in the molecular dynamics of particles to separate them across nanopores. We investigate a simplified model for an “active pore” where gating is dynamically controlled, and mimic to some extent a minimal Maxwell demon process. This model points to a rich variety of behaviors in terms of dynamical selectivity, and unravels the basic principles of active sieving [2]. We give preliminary results of a nanoscale experiment counterpart. We also solve completely a model for an “active channel” where the channel boundaries are dynamically controlled, and find yet broader perspectives on dynamical sieving. These results are corroborated by molecular dynamics simulations of water confined between flexible graphene sheets. All these principles could be readily mimicked using existing technologies to build alternatives for advanced water recycling.

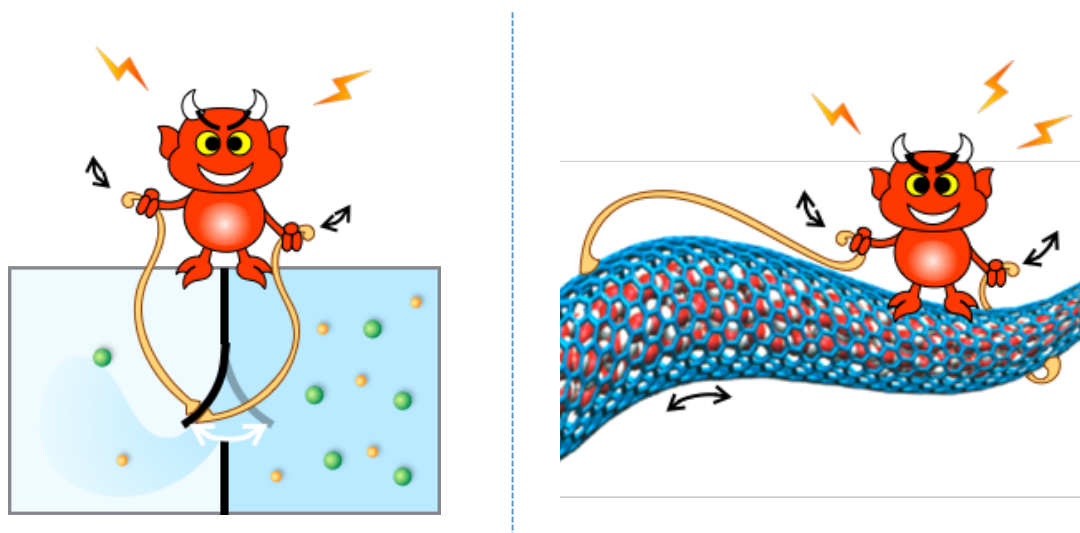


Figure 1: (left) Active sieving can be thought of in terms of a door that is mechanically opened and closed by some “crazy” Maxwell Demon and impacts the transport of particles through the door according to their dynamical properties. (right) Active sieving can also be thought of in the longitudinal direction, for instance in actively vibrating nanotubes (the vibrations being excited vibrations of the nanotube itself).

References

- [1] “Materials for next-generation desalination and water purification membranes“ Werber, J, Osuji, C. and Elimelech M., *Nature Rev. Mater.* (2016)
- [2] “Active sieving across forced nanopores for tunable selectivity “, Marbach, S and Bocquet, L., *J. Chem. Phys.* (2017).

Thermo-osmosis : is it possible to desalinate water using thermal gradients ?

L. Fu^a, S. Merabia^a, L. Joly^a

^a*Institut Lumière Matière, CNRS, Université de Lyon, Université Claude Bernard Lyon 1, 69622 Villeurbanne, France*

Key words : thermo-osmosis, water desalinization, molecular dynamics

The development of sustainable alternative energies is one of the greatest challenges faced by our society, and nanofluidic systems could contribute significantly in that field [1]. For instance, nanoporous membranes subject to a salinity gradient generate an electric current [2]. Similarly, membranes could be used to harvest energy from waste heat [3, 4]. Membranes with microscale porosity have been successfully used to generate pressure gradients under small temperature differences [5], but waste heat harvesting with nanoporous membranes has been much less explored. Using molecular dynamics simulations, we measured the thermo-osmosis coefficient by both mechanocaloric and thermo-osmosis routes, against different solid-liquid interfacial energies. We show that a modified Derjaguin's formula [6, 7] which takes into account the interfacial hydrodynamic conditions describes well the simulation results. For a non-wetting surface, thermo-osmosis transport is controlled and largely amplified by the existence of a slippage at the interface. Whereas for a wetting surface, the position of the hydrodynamic shear plane plays a key role in the determination of thermo-osmosis coefficient. The thermo-osmosis coefficient decreases for increasing wettability and a change of sign is clearly observed. Finally, in spite of a hydrodynamic backflow induced by hydrodynamic entrance effects, we found a fast thermo-osmotic flow velocity in carbon nanotube systems, which could be used to desalinate water.

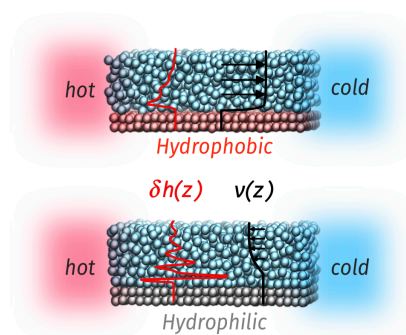


FIGURE 1 : Illustration of the thermo-osmosis flow

Références

- [1] Bocquet, L. and Tabeling, P. Physics and technological aspects of nanofluidics. *Lab on a Chip* 14, 3143–3158 (2014).
- [2] Bocquet, L. and Charlaix, E. Nanofluidics, from bulk to interfaces. *Chemical Society Reviews* 39, 1073–1095 (2010).
- [3] Barragán, V. M. and Kjelstrup, S. Thermo-osmosis in Membrane Systems : A Review. *Journal of Non-Equilibrium Thermodynamics* 42, 79 (2017).
- [4] Straub, A. P. and Elimelech, M. Energy Efficiency and Performance Limiting Effects in Thermo-Osmotic Energy Conversion from Low-Grade Heat. *Environ. Sci. Technol.* 51, 12925–12937 (2017).
- [5] Straub, A. P., Yip, N. Y., Lin, S., Lee, J. and Elimelech, M. Harvesting low-grade heat energy using thermo-osmotic vapour transport through nanoporous membranes. *Nature Energy* 1, 16090 (2016).
- [6] Derjaguin, B. V., Churaev, N. V. and Muller, V. M., *Surface Forces*, 369–431, Springer, US, (1987).
- [7] Fu, L., Merabia, S. and Joly, L. What Controls Thermo-osmosis? Molecular Simulations Show the Critical Role of Interfacial Hydrodynamics. *Phys Rev Lett* 119, 606 (2017).

Viscosity of supercooled water and two-state interpretation of water anomalies

B. Issenmann^a, A. Dehaoui^a, L. P. Singh^a, R. Berthelard¹, F. Caupin¹

^a *Univ Lyon, Université Claude Bernard Lyon 1, CNRS, Institut Lumière Matière, F-69622, VILLEURBANNE, France*

Key words: Supercooled water, Viscosity measurement, Differential Dynamic Microscopy

Although being a familiar liquid, water exhibits many anomalies, that are magnified in supercooled water (*i.e.* kept liquid below its melting point). Lowering as much as possible the volume of the sample allows reaching the lowest temperatures without crystallisation of the supercooled liquid. That is why microfluidics is particularly relevant to the study of supercooled water.

Until recently viscosity data in supercooled water were scarce [1]. We report two new viscosity experiments: one based on Brownian motion and performed at atmospheric pressure down to -34°C [2]; the other based on Poiseuille flow performed up to 300 MPa and down to 20°C below the melting line [3]. An extension of a quantitative two-state model [4] allows us to consistently describe dynamic properties of supercooled water.

References

- [1] J. Hallett, The temperature dependence of the viscosity of supercooled water, *Proc. Phys. Soc.* 82, 1046-1050 (1963)
- [2] A. Dehaoui, B. Issenmann, F. Caupin, Viscosity of deeply supercooled water and its coupling to molecular diffusion, *Proc. Natl. Acad. Sci. USA* 112, 12020-12025 (2015)
- [3] L. P. Singh, B. Issenmann, F. Caupin, Pressure dependence of viscosity in supercooled water and a unified approach for thermodynamic and dynamic anomalies of water, *Proc. Natl. Acad. Sci. USA* 114, 4312-4317 (2017)
- [4] V. Holten and M.A. Anisimov, Entropy-driven liquid-liquid separation in supercooled water, *Sci. Rep.* 2, 713 (2012)

Invited conference (III)

From microfluidic technology to organ-on-a-chip platforms: new opportunities to develop physiologically relevant *in vitro* models

S. Le Gac

Applied Microfluidics for BioEngineering Research, MESA+ Institute for Nanotechnology, MIRA Institute for Biomedical Engineering and Technical Medicine, University of Twente, The Netherlands

Key words: organ-on-a-chip models, nanomedicine, multicellular tumor spheroids, assisted reproductive technologies

1. Introduction

Lab-on-a-chip technology (LOC) has reached a mature state and has become highly popular for life sciences, due to the numerous advantages it offers. While microfluidic developments have initially been driven by the field of bioanalysis, LOC applications have been extended to cell experimentation, for which LOC technology presents additional advantages: an *in vivo*-like and tunable microenvironment, dynamic culture, and a unique capability to couple cell culture, treatment and analysis on one single platform. In this presentation, I will particularly discuss two applications of microfluidics, in the fields of assisted reproductive technologies (ART) and cancer research.

2. Microfluidics for assisted reproductive technologies (ART)

In the field of ART, LOC technology offers alternative approaches for all *in vitro* steps of the treatment, to eventually remedy currently encountered issues [1]. So far, we have focused on two steps, the pre-implantation *in vitro* culture of embryos, and (ii) their characterization, to monitor their growth and identify embryos with the highest developmental competence before transfer. A first microfluidic platform was developed and validated on mouse embryos, demonstrating that microfluidic chambers support the full-term development of mouse embryos down to the single embryo level, with birth rates comparable to group culture in a conventional format (droplet culture) [2]. After upgrade, the device was tested on donated frozen human embryos [3]. Next, an electrochemical sensor has been developed, together with an original measurement protocol, to monitor in real-time variations in the dissolved oxygen concentration in the culture chamber [4]. Current work concerns the integration of the sensor in the culture device.

3. Tumor-on-a-chip models – evaluation of nanomedicine delivery and penetration

For drug screening, and to evaluate the penetration and efficiency of nanomedicines, sophisticated and biomimetic *in vitro* models are required that incorporate essential features of the tumor microenvironment. In that context, we are developing a tumor-on-a-chip platform that relies on the use of 3D tumor models (spheroids) [5] prepared from either a mono-culture (breast tumor cells) or a co-culture (breast tumor cells and fibroblasts), to yield a model closer to the *in vivo* situation [6]. In our first generation platform, spheroids are trapped in a microfluidic chamber, and this platform has been applied to evaluate the penetration of fluorescently nanoparticles, employed here as surrogates for nanomedicines, under either static conditions or flow. A second generation platform is under development, where the 3D tumor model is combined to a vascular system for the delivery of the drugs/nanomedicines to the tumor site.

References

[1] Le Gac & Nordhoff, Microfluidics for mammalian embryo culture and selection: where do we stand now?, *Molec. Human Reprod.*, 23, 213-226 (2017); [2] Esteves et al., Microfluidic system supports single mouse embryo culture leading to full-term development, *RSC Adv.*, 3, 26451-26458 (2013); [3] Kieslinger et al., *In vitro* development of donated frozen thawed human embryos in a prototype static microfluidic device: a randomized controlled trial, *Fertil. Steril.*, 103, 680-686 (2015); [4] van Rossem et al., Sensing oxygen at the millisecond time-scale using an ultra-microelectrode array (UMEA), *Sens. Act. A.*, 238, 1008-1016 (2017); [5] Sridhar et al., Microstamped Petri dishes for scanning electrochemical microscopy analysis of arrays of microtissues, *Plos One*, 9, e93618 (2014); [6] Priwitaningrum et al., Tumor stroma-containing 3D spheroid arrays: A tool to study nanoparticle penetration, *J. Control. Release*, 244, 257-268 (2016).

Lab on Chip

DEVELOPMENT OF A MICROFLUIDIC BIOMIMETIC DEVICE FOR TRIPLE NEGATIVE BREAST CANCER STEM CELLS EXTRAVASATION STUDIES

A.SIVERY¹, J. DUVAL², V.SENEZ¹, X. LEBOURHIS^{2,3}, C. LAGADEC^{2,3} and A. TREIZEBRE¹

¹Univ. Lille, CNRS, Centrale Lille, YNCREA ISEN, Univ. Valenciennes, UMR 8520-IEMN Lille, France

²CPAC, Cell Plasticity and Cancer, Univ. Lille, INSERM U908 Villeneuve d'Ascq, France

³SIRIC OncoLille, Lille, France

KEY WORDS: Cancer Stem Cell (CSC), Circulating Tumor Cells (CTC), Biomimetic Microfluidic device, Extravasation, Tumor On Chip

1. Introduction

Since several years, the discovery of a population of CSCs within tumors has altered our conception of cancer organization and treatment responses [1]. CSCs are suspected of being involved in the metastatic cascade that results in the emergence of distant secondary tumors. Interestingly, the most aggressive of cancers, the triple negative breast cancers (TNBC) is the subtype containing the highest amount of CSC [2]. We want to assess if metastases arise from circulating CSCs able to extravasate and resume growth and/or if metastases arise from 'non-CSC' Circulating Tumor Cells (CTC) that will reprogram as CSCs once extravasated in appropriate environment [3].

2. Microfluidic device

This device, fabricated in silicone elastomer (PDMS), is composed of two chambers. The first is dedicated to reproduce a microvasculature network mimicking the configuration of natural blood vessels [4] and the second to generate a specific modifiable metastatic niche or to apply the chemo-attraction stroma (Fig.1). In the top layer, the entrance channel is 800 μm wide. Each channel, of 50 μm of deep, are divided into two half-width channels, up to 8 channels of 100 μm in the center of the device. The bottom layer is composed of a channel, 1mm wide and 150 μm thick placed under each top channel. These chamber layers are separated by SU8 porous membrane with pores sizes of 10 μm (Fig.2).

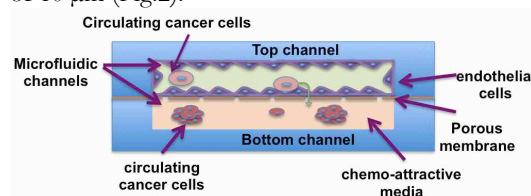


Figure 1: Cross section of the microfluidic device

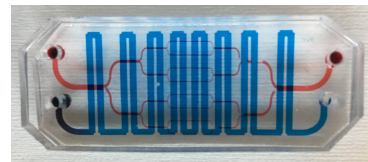


Figure 2: Photo of the microfluidic PDMS device filled with red ink (top channel) and blue ink (bottom channels).

3. Results

We have successfully generated 3D biomimetic blood vessels in a reproducible manner. Briefly, channels inner surface are coated with fibronectin (50 $\mu\text{g}/\text{ml}$) and collagen (100 $\mu\text{g}/\text{ml}$). Then, Human Umbilical Vein Endothelial Cells (HUVECs) are injected at high density (8.105 cells in 15 μl) in the top chamber and cell culture medium (EGM-2) is perfused during 3 days to allow for cells adhesion and proliferation (Fig.3). We have also evaluated cancer cell attachment on HUVECs monolayer. For this, HUVECs monolayer was first activated with 10 ng/ml TNF-Alpha for 24 h. Then, human breast adenocarcinoma cells (MDA-MB-231) were injected inside the top channel under flow (2 to 10 $\mu\text{l}/\text{min}$). Our preliminary results showed that a sub-population of cells remained attached to the activated endothelial monolayer (Fig.4).

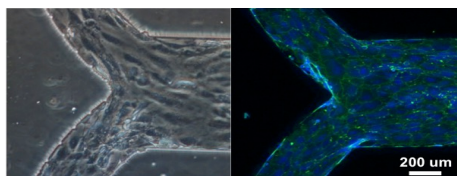


Figure 3: Image of transmission microscopy in phase contrast (left). Fluorescence microscopy image (right): Hoechst staining (blue) and anti-CD31 staining (green)

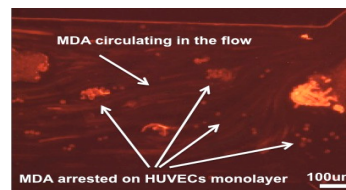


Figure 4: MDA cells perfused activated HUVECs monolayer

Our next step is to keep media flowing to long-term study attached cells extravasating and collect extravasated cells through the bottom channels and non-extravasated cancer cells through the upper channels in order to study their phenotype (CSC). Our ultimate goal is to modify bottom chamber environment and identify its impacts on extravasation, CSC phenotype and ability to develop secondary tumors.

References

- [1] Al-Hajj & al. "Prospective identification of tumorigenic breast cancer cells." Proc. Natl. Acad. Sci. U.S.A. 100, 3983–3988, 2003.
- [2] Atkinson R.L. & al. "Cancer stem cell markers are enriched in normal tissue adjacent to triple negative breast cancer and inversely correlated with DNA repair deficiency". Breast Cancer Res. 15(5):R77, 2013.
- [3] Guler G. & al. "Stem cell-related markers in primary breast cancers and associated metastatic lesions". Mod. Pathol. 25, 949–955, 2012.
- [4] Tsai M. & al. "In vitro modeling of the microvascular occlusion and thrombosis that occur in hematologic diseases using microfluidic technology", J Clin Invest. 408-418, 2012.

Microfluidic platform to restore the angiogenic balance in preeclampsia

L. Alexandre^{a,b,c}, L. Trapiella Alfonso^d, N. Eilstein^d, J. Guibourdenche^e, E. Lecarpentier^f, V. Tsatsaris^f, J-L. Viovy^{a,b,c}, L. Malaquin^g, S. Descroix^{a,b,c}

^aInstitut Curie, PSL Research University, CNRS, UMR 168, F-75005, Paris, France

^bSorbonne Universités, UPMC Univ Paris 06, CNRS, UMR 168, F-75005, Paris, France

^cInstitut Pierre Gilles de Gennes, 75005 Paris, France

^dUMR8638-CNRS – Université Paris Descartes, Faculté de Pharmacie, Sorbonne Paris Cité, Paris, France

^eHormonology & perinat collection equipex platform, Centre hospitalier universitaire Cochin Broca-Hôtel-Dieu, Groupe hospitalier universitaire Ouest, AP-HP, Paris, France

^fDépartement de gynécologie obstétrique I, Maternité Port-Royal, Centre hospitalier universitaire Cochin-Broca-Hôtel-Dieu, Groupe Hospitalier Universitaire Ouest, AP-HP, Paris, France

^gLAAS-CNRS, 31031 Toulouse, France

Keywords: microfluidic fluidized bed, magnetic beads, preeclampsia, apheresis, angiogenic factors

1. Introduction Preeclampsia is a hypertensive disorder of pregnancy linked to placenta insufficiency, and associated to extreme prematurity. It is currently considered that preeclampsia is connected with maternal endothelial dysfunction due to the excess or the lack of angiogenic factors such as sFlt-1 (soluble Fms-like tyrosine kinase 1) and PlGF (placental growth factor) into the maternal circulation [1]. Clinical studies have shown the involvement of the sFlt-1/PlGF ratio in the syndrome of preeclampsia and its correlation with the severity of the disease [2]. Restoring the angiogenic balance is a solution to delay the birth of an extremely preterm infant and increase from 10% to at least 30% his or her chances of survival without sequelae.

In this context, we present here a microfluidic extra corporal technology as a platform to screen strategies to remove factors that play a causative role in the pathophysiology of preeclampsia. Our team developed a system of micro-fluidized bed, based on the equilibrium between two forces: a drag force created by the fluid that flows inside the micro-chamber of the system and a magnetic force that maintains the particles in the micro-chamber under the hydrodynamic flow [3]. This very special configuration enhances transfer between a fluid and the surface of the beads, with low back pressure and reduced risks of clogging. By grafting specific ligands on the surface of the beads, we can use this asset to capture a target present in the sample flowing through the bed. This system has already shown its efficiency in many fields of application [4]. We present here an innovative approach to restore the angiogenic balance by a competitive bioassay that allows capturing the protein sFlt-1 in excess while releasing its ligand PlGF in default.

2. Methods PDMS chips were made by pouring polydimethylsiloxane (PDMS, Sylgard 184, Dow Corning) on brass molds produced by micro-milling. The bonding was performed through oxygen plasma. Surface treatment was performed using PDMA-AGE 0.5% (w/v), with one hour incubation. Magnetic field is created by a NdFeB 1.47 T permanent magnet positioned at 1.5 mm from the chip. Control of the flow was performed using Fluigent systems such as MAESFLO controller and flow unit. Beads used were coated with VEGF (Vascular Endothelial Growth Factor) at 35% using streptavidin-biotin interaction. Experiments were performed on culture supernatants of human trophoblastic cells and pools of maternal plasma. Concentrations of growth factors were measured by immunoassays at the hormonology laboratory at Cochin hospital.

3. Results To shift the equilibrium of sFlt-1-PlGF binding, we coated the surface of magnetic beads with a competitive ligand (VEGF). The microfluidic system has been developed to optimize the interaction of sFlt-1 with the functionalized magnetic beads. We demonstrate its ability to capture it specifically (up to 46% \pm 1 of capture) at rates similar to those obtained on batch (52% \pm 5) in both matrices of culture supernatant and pool of maternal plasma. Compared to classical apheresis columns [5], the nonspecific absorption is completely controlled (<3%). Using our competitive biomimetic binding approach, the ligation of sFlt-1 increases the bioavailability of PlGF. We were able to show a decrease of 83% of the ratio sFlt-1/PlGF from original samples at preeclamptic growth factors concentrations, leading to a final sample with a healthy ratio (lower than the clinical limit).

Conclusion We demonstrate an alternative way to restore the angiogenic balance thanks to a competitive approach, in order to delay the birth of an extremely preterm infant. This approach has been adapted from culture supernatant to more complex matrices, such as pool of maternal plasma.

References: [1] Sibude J and al. *Placental growth factor for the prediction of adverse outcomes in patients with suspected preeclampsia or intrauterine growth restriction*. PLoS One, 7, 11 (2012)

[2] Levine RJ *Circulating angiogenic factors and the risk of preeclampsia*. N Engl J Med. 350:672-683 (2004)

[3] Iago Pereiro and al. *Magnetic fluidized bed for solid phase extraction in microfluidic systems* Lab Chip, 17, 1603-1615 (2017)

[4] Iago Pereiro and al. *A new microfluidic approach for the one-step capture, amplification and label-free quantification of bacteria from raw samples* Chem. Sci., 8, 1329-1336 (2017)

[5] Thadhani R and al. *Pilot study of extracorporeal removal of soluble fms-like tyrosine kinase 1 in preeclampsia* Circulation. 23;124(8):940-50 (2011)

Microbes under pressure

L. Holt^a, O. Hallatschek^b, M. Delarue^c

^a*Institute for Systems Genetics, NYU Medical Center, NY, USA*

^b*Physics Department, University California, Berkeley, USA*

^c*MILE, LAAS-CNRS, Toulouse, France*

Key words: microfluidics, microbiology, mechanical stress

Cells act upon the elastic extracellular matrix and against steric constraints when proliferating in a confined environment resulting, at the population level, in a **compressive, growth-induced, mechanical stress**. Growth-induced stress is ubiquitous to any cell population proliferating in a confined environment, whether partly or fully, such as microbes found to develop in the form of biofilms embedded in micrometer-sized pores or within biological tissues. Despite their paramount importance, **compressive mechanical stresses have been largely** unexplored in contrast to other types of mechanical stress, owing to the technical challenges of confining cells, and in particular microbes.

Microfluidics offers an arsenal of elements that are amenable for the study of microbes under spatial confinement. We developed the **first microfluidic devices that enable an acute control of the mechanical environment experienced by a microbial cell population**, while keeping the chemical environment constant [1]. Using these microfluidic devices, we elucidated a process by which a partially confined cell population could build-up growth-induced stress: **We found that when *S. cerevisiae* are grown in confinement, force chains propagate within the population and stabilizes it, resulting in a self-driven jamming**. Growth-induced pressure emerges from jamming, which is strong enough to affect the physiology of the microbes and strain their microenvironment.

We unraveled unique effects of compressive growth-induced stresses on the response of *S. cerevisiae*, impacting both global biophysical parameters and specific biological pathways. More specifically, we used a new type of nanoparticles [2] to measure that compressive cells have drastically different microrheological parameters leading to a decrease in their growth rate [3]. Moreover, we identified the first mechano-sensitive network, that we termed SCWISh, essential for cell adaptation growing in a spatially-constrained environment: the simple knockout of two genes of the SCWISh network is enough to prevent cell survival under growth-induced compressive stress [4].

Our new microfluidic approach enable for the first time the study of microorganisms under a defined mechanical and chemical environment. It opens avenues for the understanding of compressive stress on various aspects of microbial infections, from its coupling to antibiotics to drive a biological response, to the very invasion of pathogens under a given set of mechano-chemical parameters.

References

- [1] M. Delarue et al. "Self-driven jamming in growing microbial populations," *Nat. Phys.*, vol. 12, no. 8, pp. 762–766, 2016.
- [2] M. Delarue et al. "mTORC1 controls phase-separation and the biophysical properties of the cytoplasm by tuning crowding," (*in revision in Cell*)
- [3] L. Holt and M. Delarue. (*in prep*)
- [4] M. Delarue et al. "SCWISh network is essential for survival under mechanical pressure.," *Proc. Natl. Acad. Sci. U. S. A.*, vol. 114, no. 51, pp. 13465–13470, 2017.

On-chip Flow Cell Sorting System Based on High frequency Dielectrophoresis implemented on CMOS technology

R. Manczak^a, S. Saada^b, F. Hjeij^a, C. Dalmay^a, F. Lalloue^b, Mehmet Kaynak^c, A. Pothier^a

^aXLIM & ^bEA3842 Université de Limoges, Limoges, France

^cTHP microelectronic, Franckfurt Oder, Germany

Key words: dielectrophoresis, microfluidic, cell sorting, CMOS technology

1. Introduction

Isolation and characterization of Cancer Stem Cells (CSCs) is of prime important in the development of new therapeutic treatments, especially in brain cancers. Such cells present strong therapeutic resistance and are responsible for cancer recurrence [1]. The large cell heterogeneity in tumors makes identification of such cells very huge and lead to the development of alternative analysis technics. In this context, microfluidic cell sorter based on dielectrophoresis (DEP) technics have already demonstrated capabilities in the 10 kHz to 1 MHz frequency range [2]. Increasing operating frequencies, i.e. 100 MHz to 1 GHz (Ultra High Frequency band UHF) is very interesting as intracellular properties dominate the cell response [3]. This paper presents an innovating on-chip UHF DEP cell sorting system, implemented on CMOS chip coupled to microfluidics technologies enabling integration of additional capabilities with the expected frequency range and flexibility.

2. Design and Simulation of the cell sorting system

The developed cell sorter is presented in Fig. 1(a). An array of 16 electrodes are implemented on passive layers of a CMOS chip. Opposite electrodes are biased with a high frequency signal generator whereas the others are grounded to generate an appropriate electric field gradient. Hence, particles which experience positive DEP are attracted near the edge of electrodes (high intensity areas) whereas in negative DEP, particles are repelled at the center of the channel (low intensity areas).

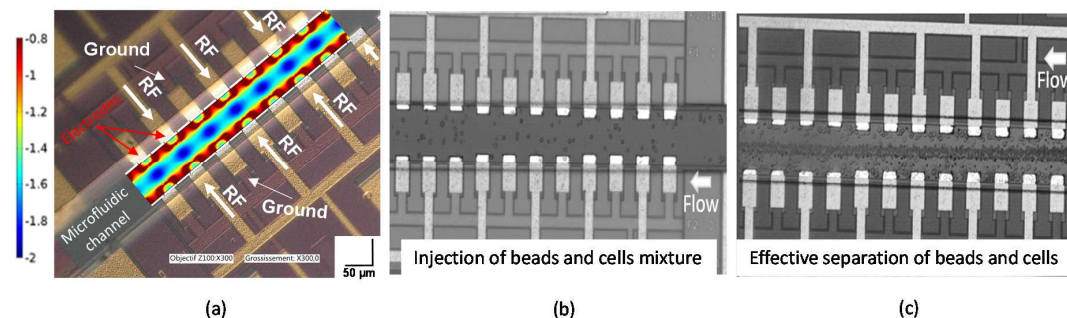


Figure 1: Photograph of the developed UHF DEP cell sorter implemented on CMOS technology with a plot of the normalized electric field (log scale) under an applied signal of 3V at 300 MHz – Photograph of the device with a mixture of LN18 cells and beads injected in the channel (b) – Photograph of the device under a 50 MHz signal applied (c).

3. Experimental Results

In order to find the appropriate working frequency to sort cells, LN18 line cells cultured with standard medium (cell line derived from malignant gliomas adult patients) have been characterized using UHF DEP characterization to determine their second cross over frequency (when the transition between positive and negative DEP occurs) around 116 MHz [3]. Then a mixture of polystyrene beads and LN18 cells are injected in the cell sorter (Fig.1(b)). Polystyrene beads exhibit negative DEP whatever the frequency range. Working at 50 MHz, lower than the cross over frequency of LN18 cells, one can see that polystyrene beads are concentrated at the center of the channel, whereas cells are located near the edges of electrodes (Fig.1(c)).

4. Conclusion

This paper demonstrates the feasibility of implemented a new type of cell sorter based on UHF DEP on CMOS technology allowing to envision to integrate power sources and active readout circuitry on chip.

References

- [1] H.M. Jeon, S.H. Kim, X. Jin, J.B. Park, S.H. Kim, "Crosstalk between Glioma-Initiating Cells and Endothelial Cells Drives Tumor Progression", *Cancer Research*, 74, 16, pp. 4482-4492 (2014).
- [2] A. Valero, T. Braschler, T. Renaud, "A Miniaturized Continuous Dielectrophoretic Cell Sorter and Its Applications", *Biomechanics*, 4, 2 (2010).
- [3] F. Hjeij, C. Dalmay, B. Bessette, G. Begaud, *et al.*, "Biological Cell Discrimination Based on Their High Frequency Dielectrophoretic Signatures at UHF Frequencies", *IEEE MTT-S Microwave Symposium* (2017).

Simple optimization of single-level particle trapping flow-through microfluidic devices using oblique hydrodynamic flow

O. Mesdjian^{a,b}, K. Sakai^{a,b}, J. Fattaccioli^{1,2,3*}

^aPASTEUR, Département de chimie, École normale supérieure, PSL University, Sorbonne Université, CNRS, 75005 Paris, France

^bInstitut Pierre-Gilles de Gennes pour la Microfluidique, 75005 Paris, France

Key words: microfluidic trapping, microfabrication, colloidal particles

With the aim to monitor physico-chemical or biological processes, a strong effort has been put these last years to develop microfluidic devices [1,2] for the control of the spatial positioning of small objects such as cells or droplets [3,4], to allow their analysis over various timescales, at the single object level, alone or in interaction with other cells [5] or particles.

Over the wide range of hydrodynamic devices that have been developed so far, flow-through microsystems can be composed of auxiliary channels regularly spaced perpendicularly to a serpentine main channel [6], or arrays of half-circular [7] or U-shaped [3] trapping pocket. In this latter case, trap arrays were fabricated by single layer soft lithography [8], and could be improved in terms of efficiency, by making standing traps from double layer lithography [9,10], or in terms of selectivity, using reverse flow loading to immobilize multiple similar or different objects [4,10] together. Despite their simple fabrication process, single-level trapping arrays are generally less efficient than their double-level counterparts, since both the amount and the velocity of the fluid carrier entering the traps and escaping from their backside openings is much smaller than for the main flow, thus diminishing the probability for a trap to capture a particle.

In this work, we address this issue by showing that, contrary to the existing examples of single-level trapping devices from the literature that uses hydrodynamic flows parallel to the trap array, skewing the main direction of this flow increases both the efficiency and the spatial homogeneity of trapping at the full chip level. After a brief description of the fabrication process of the microfluidic traps and both the straight and skewed devices, we quantify and compare the trapping kinetics and homogeneity using model particles having sizes comparable to cells. Then, we show that mammalian cells can be efficiently immobilized using the skewed configuration. Finally, using simple simulations we will try to qualitatively explain the striking difference between the behavior of the straight and skewed configuration.

References

- [1] V. Narayanamurthy, S. Nagarajan, A. Y. Firus Khan, F. Samsuri, and T. M. Sridhar, *Anal. Methods* **9**, 3751 (2017).
- [2] J. Nilsson, M. Evander, B. Hammarström, and T. Laurell, *Anal. Chim. Acta* **649**, 141 (2009).
- [3] A. Huebner, D. Bratton, G. Whyte, M. Yang, A. J. deMello, C. Abell, and F. Hollfelder, *Lab Chip* **9**, 692 (2009).
- [4] Y. Bai, X. He, D. Liu, S. N. Patil, D. Bratton, A. Huebner, F. Hollfelder, C. Abell, and W. T. S. Huck, *Lab Chip* **10**, 1281 (2010).
- [5] B. Dura and J. Voldman, *Curr. Opin. Immunol.* **35**, 23 (2015).
- [6] W.-H. Tan and S. Takeuchi, *Proc. Natl. Acad. Sci. U. S. A.* **104**, 1146 (2007).
- [7] D. Di Carlo, L. Y. Wu, and L. P. Lee, *Lab Chip* **6**, 1445 (2006).
- [8] Y. Zhou, S. Basu, K. J. Wohlfahrt, S. F. Lee, D. Klennerman, E. D. Laue, and A. A. Seshia, *Sensors Actuators, B Chem.* **232**, 680 (2016).
- [9] D. Di Carlo, N. Aghdam, and L. P. Lee, *Anal. Chem.* **78**, 4925 (2006).
- [10] A. M. Skelley, O. Kirak, H. Suh, R. Jaenisch, and J. Voldman, *Nat. Methods* **6**, 147 (2009).

Posters (II)

Monolithic fabrication of glass suspended microchannel resonator for enhanced biosensing application

Roberta Calmo^a, Andrea Lovera^b, Stefano Stassi^a, Alessandro Chiadò^a, Francesca Bosco^a, Carlo Ricciardi^a

^a Department of Applied Science and Technology, Politecnico di Torino, Corso Duca degli Abruzzi 24, 10128 Torino, Italy

^b FEMTOprint S.A, Via delle Industrie 3, 6933 Mugello, Switzerland

Key words: Monolithic fabrication, suspended microchannel resonator, biosensing

Resonating micromechanical structures have been recently developed as highly sensitive platform to study how drugs affect cells growth [1, 2, 3]. Unfortunately the time-consuming and challenging fabrication process [4] represents the main drawback for the implementation of these platforms in new point-of-care devices.

In this work, we present an innovative and rapid fabrication process, of totally transparent suspended microchannel resonator (SMR), based on the femtosecond laser direct writing [5]. By using this new approach it was possible to fabricate the resonant structure and the integrated microfluidic system in one-step (Figure 1a).

The SMR shows remarkable mass and density resolution (0.14 pg and 0.001 kg/m³ respectively), comparable to state of art SMR silicon based sensors [6, 7]. These values were evaluated by the means of a calibration curve correlating the frequency response (Figure 1b) in function of the density of different fluids flushed inside the suspended microchannel. Once the device was mechanically characterized, the effective biosensing capability has been demonstrated by evaluating the microbial load of aqueous solutions containing different concentrations of *P. fluorescens*. The unique transparency of the SMR provides the opportunity of combining mechanical and optical characterizations for direct monitoring of bacteria activity and drug resistance.

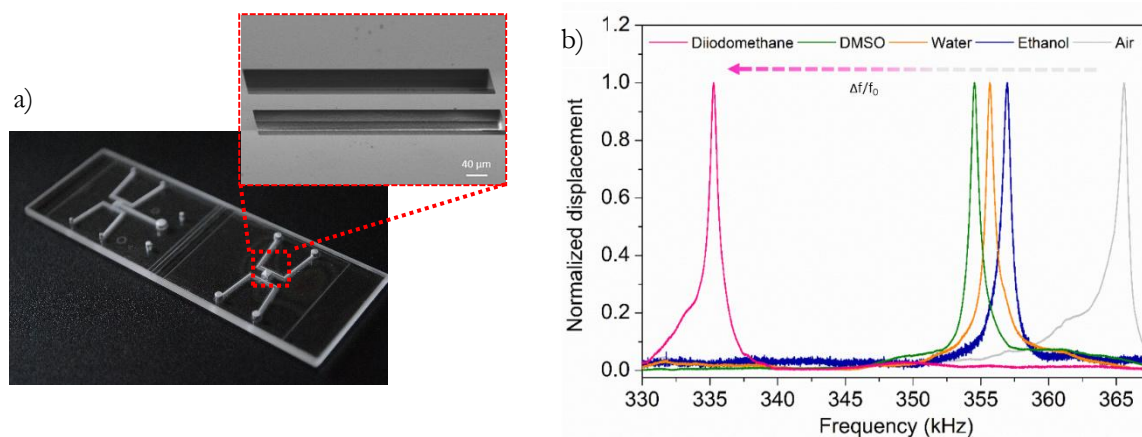


Figure 1: a) The SMR integrated with the microfluidic system; b) evaluation of the capability of the SMR to distinguish liquid characterized by different density.

References

- [1] N. Cermak et al. Nature biotechnology, 2016, 34, 1052-1059
- [2] J. Lee et al., Nano Letters 2010, 10, 2537–2542
- [3] M.M. Stevens et al., Nature biotechnology, 2016, 34, 1161-1167
- [4] T.P. Burg et al., Physical review letters, 2009, 102, 228103
- [5] Y. Bellouard et al., Journal of Laser Micro / Nanoengineering, 2012, 7, 1-10
- [6] M. F. Khan et al., Sensor and Actuators B:Chemical, 2013, 185, 456-461
- [7] D. Lee et al., Scientific Reports, 2016, 6, 33799

Fluid-particle coupling induced micro-magnetic trapping of highly diffusive magnetic nano-particles

M. Fratzl^{a,b}, G. Blaire^a, S. Delshadi^{a,c}, T. Devillers^b, F. Bruckert^d, O. Cugat^a, and N. M. Dempsey^b

^aUniv. Grenoble Alpes, CNRS, Grenoble INP, G2Elab, 38000 Grenoble, France

^bUniv. Grenoble Alpes, CNRS, Grenoble INP, Institut Néel, 38000 Grenoble, France

^cUniv. Grenoble Alpes, CNRS, Inserm, IAB, 38000 Grenoble,

^dUniv. Grenoble Alpes, CNRS, Grenoble INP, LMGP, 38000 Grenoble, France

Key words: Magnetophoresis, Nanoparticles, Droplets

Millimeter sized magnets are often used to trap magnetic particles in microfluidic setups for the manipulation of biological elements (cells, molecules...) [1]. As the field gradient values emitted by such magnets are somewhat limited (10^3 - 10^4 T/m), particles of relatively large volume (1 μm diameter or more) have typically been used to overcome Brownian force. In this work, we propose the use of micro-magnets producing magnetic field gradients as high as 10^6 T/m [2] have been used to efficiently trap nanoparticles with a magnetic core of just 12 nm in diameter, with previous studies suggesting that such particles cannot be permanently captured [3]. Particle capture efficiency increases with increasing particle concentration. Comparison of measured capture kinetics with numerical modelling reveals that a threshold nanoparticle concentration exists below which capture is diffusion-driven and above which it is convectively-driven. It also shows that two-way fluidparticle coupling is responsible for the formation of convective cells, the size of which is governed by the height of the droplet. Our results indicate that for a suspension with a nanoparticle concentration suitable for bioassays (of the order of 0.25 mg.ml^{-1}), all particles can be captured in less than 10 minutes. The efficient capture of nanoparticles having a significantly higher surface to volume ratio than the more widely used microparticles, should contribute to the development of next generation digital microfluidic Lab-on-Chip immunoassays.

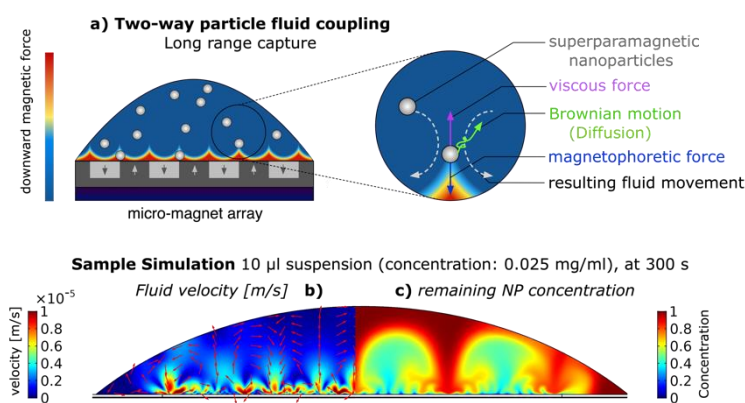


Figure 1: Nanoparticles will be captured at the junctions between micro-magnets, accelerating their surrounding fluid (a). Numeric simulation shows that the nanoparticles attracted by micro-magnets will drag the fluid towards the magnetic array (b). There, the suspension will be depleted and the fluid will flow back to the top of the droplet, eventually pushing more nanoparticles toward the magnetic junction. This bi-directional magnetic-viscous coupling leads to a self-organization of the suspension (magnetophoretic convection) (b), finally resulting in efficient trapping of highly diffusive particles.

References

- [1] M. A. M. Gijs et al., Microfluidic applications of magnetic particles for biological analysis and catalysis, Chem. Rev. 110, 1518-1563 (2009).
- [2] F. Dumas-Bouchiat, et al., Thermomagnetically patterned micromagnets,” APL 96, 102511 (2010).
- [3] M. Colombo, et al., Biological applications of magnetic nanoparticles, Che. Soc. Rev. 41, 4306 (2012).

PRODUCTION OF BIOSOURCED FOAMS BY MICROCHANNELS AT HIGH THROUGHPUT

Julian Sepulveda ¹, Agnès Montillet ¹, Dominique DellaValle ², Catherine Loisel ^{2,3},
and Alain Riaublanc ⁴

¹ GEPEA, Université de Nantes, France.

E-mail: julian.sepulveda@oniris-nantes.fr

² ONIRIS, France. ³ GEPEA, ONIRIS, France. ⁴ BLA, INRA, France

Key words: foaming, millifluidics, foam structure

In recent years, the use of microchannels has emerged as an interesting alternative to produce emulsions and foams with uniform and controlled size distribution of bubbles and droplets [1]. A previous study [2] has shown the potential of microchannels in terms of research and development as well as industrial applications.

During that study, differences in the foam structure were found between the moment of foam formation and the final product. The changes of geometry throughout the process before obtaining the final product are thought to be at the origin of this foam structure evolution.

Therefore, the aim of this study was to evaluate the effect that geometrically modified microchannels may have on foam structure. Similarly, the effect of the liquid base viscosity as well as the liquid flowrate used are evaluated. Significant differences have been found for these factors and their interactions.

Figure 1. shows the results at two liquid flowrates for the elastic module (G') when using two microchannel configurations (CX600 and CX-E600) and a liquid base at two different viscosities (WPI3XG02 and WPI3XG04). Foams with different degrees of stiffness have been found leading to the conclusion that microchannel configuration have an impact on foam structure.

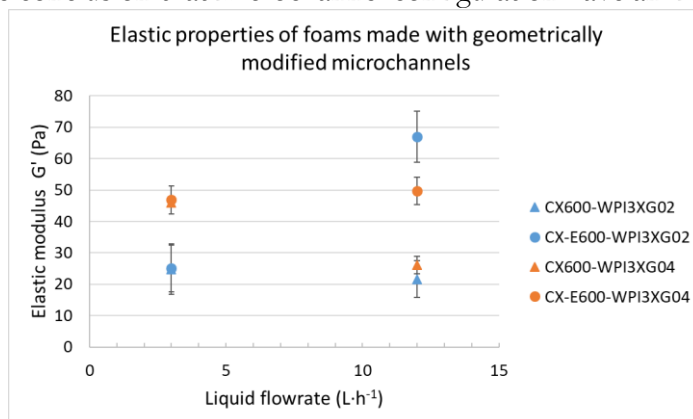


Figure 1. Rheological response of foams produced using two different microchannel configurations and a liquid base at two viscosities.

References

- [1] Anna, S. L. (2016). Droplets and Bubbles in Microfluidic Devices. *Annual Review of Fluid Mechanics*, 48(1), 285–309.
- [2] Laporte, M. (2014) *Étude de l'écoulement diphasique à l'échelle millimétrique et micrométrique : application aux mousses*. PhD Thesis. Faculté des sciences et des techniques, Université de Nantes, France.

Utilizing a Molecular Program for the Hypersensitive Detection of Nucleic Acids

Roberta Menezes¹, Guillaume Gines², Valerie Taly¹ and Yannick Rondelez²

¹INSERM UMR-S1147, CNRS SNC5014, Paris Descartes University, Paris. Equipe labellisée Ligue Nationale contre le cancer. ²UMR 7083, ESPCI, 10 Rue Vauquelin 75005 Paris.

Key words: droplet microfluidics, liquid biopsy, molecular programming, disease biomarkers

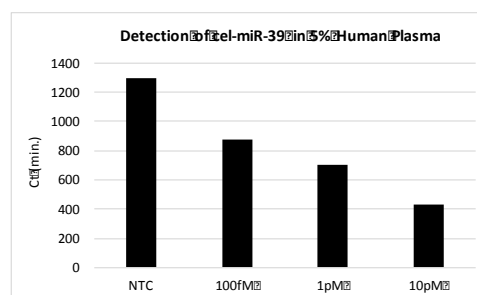
1. Introduction

An emerging new method for detecting biomarkers, involves the profiling of circulating nucleic acids (CNA), as early-stage, minimally invasive diagnosis (2). However, detection can be challenging, because they may have very short sequences, high sequence homology and are also present in low concentrations in the blood. The tools used to profile them need to be sensitive, specific and quantitative.

2. Detection System

Here we present a molecular program in the form of an in vitro nucleic acid circuit, designed to detect specific target sequences. This system is then combined with droplet microfluidics to provide absolute quantification of the target, similarly to digital PCR. According to the Poisson law, only droplets containing the target will fluoresce, so the original target copy number in the sample can be calculated. The detection program is a self-organized dynamic system rationally designed with a standardized set of templates, enzymes and dNTPs as fuel. These components interact with each other to emit a strong fluorescent signal, in the presence of a single copy of target sequence. This detection method has several advantages over the current gold-standard RT-qPCR. It is an isothermal 1-step reaction. It is also less prone to background signaling. And combining it to droplet based microfluidics provides absolute quantification and does not require calibration or internal controls. Our results thus far show we can successfully detect synthetic targets in human plasma background (Figure).

Figure: Detection of cel-miR-39 concentration range spiked in 5% human plasma extract. Ct values correspond to 0.5 normalized RFU.



References

[1] Montagne, *et al.*. Boosting functionality of synthetic DNA circuits with tailored deactivation. *Nature Communications*, 7, 13474 (2016)

[2] Pekin, *et al.* Quantitative and sensitive detection of rare mutations using droplet-based microfluidics. *Lab on a Chip*, 13 (2011)

Active matter in complex media

M. Brun-Cosme-Bruny, S. Rafai, P. Peyla

Key words: microswimmer, random walk, diffusivity, hydrodynamic interactions

1. Introduction

The microalga *Chlamydomonas Reinhardtii* is used here as a model microswimmer to study the effect of complex environments on its swimming. Its motion can be modeled by a persistent random walk where we can extract an analogous diffusion coefficient. In our experiments, we model a complex medium by a series of microfabricated pillars. Their diffusivity is analysed by means of particle tracking. Relevant statistical observables allowed us to quantify the bias involved by the presence of pillars as a function of pillars density. Particularly, as the interpillar-distance is shortened, the mean correlation time of direction gets shorter, so does the diffusion coefficient. This provides the first bases of understanding on active matter in complex environments.

LEDECOCK^a C. KEITA^a M. SCHLENK^b I. B. SALMON^{*,a}

4. CHIPS 6.1. LOF LUTB 5250 H: D. 1. F 22600 D. F. F. 4

$$1 \leq i \leq n, \quad 1 \leq j \leq m, \quad 1 \leq k \leq l, \quad 1 \leq p \leq q, \quad 1 \leq r \leq s, \quad 1 \leq t \leq u, \quad 1 \leq v \leq w, \quad 1 \leq x \leq y, \quad 1 \leq z \leq \infty$$

\mathbb{P}^1 : $1GL$: $1LH$: $16P$: $1D95440P$: $1C$

We report the fabrication of highly permeable membranes in poly(ethylene glycol)



[11] Lee et al. *Biomacromolecules* 2010, 11, 3316

Portable microfluidics based on hyperelastic materials

C. Parent¹, L. Davoust², J.L. Achard³, G. Gropplero¹, Y. Fouillet¹

¹ CEA LETI MINATEC Campus, Univ. Grenoble F-38054 Grenoble, France

² Grenoble-INP/Univ. Grenoble-Alpes, SIMaP, 38402 Saint Martin d'Hères, France

³ CNRS, Univ. Grenoble-Alpes, LEGI, 38051 Grenoble Cedex 9 France

Key words: Microfluidics, hyperelastic, stretchable, Lab On a Chip, polymeric foam

Following the development of microfluidic systems in the last decades, there has been a high tendency towards developing lab-on-a-chips with the goal of performing biochemical assays on a consumable fluidic chip connected to portable platforms for point of care applications. In this field, many kinds of microfluidic systems are fabricated from soft silicon (PDMS) that makes the integration of microvalves and micropumps [1] easier. More recently, materials that exhibit deformability capabilities much larger than the one of PDMS have been introduced in different growing applications such as soft robots [2] or sensors [3].

The purpose of this work is to demonstrate how hyperelastic materials can address some challenges in the field of point-of-care applications. A first illustration is given here based on a new digital microfluidics approach which involves collapsible chambers using a stretchable membrane for addressing complex protocols (ELISA). An elastomer is a key material with which the chambers, having a large range of volume (μl to few $100\mu\text{l}$), can be filled and emptied totally at low pressures (few hundreds of mbar) using a portable pneumatic instrumentation (Fig1-right).

A second illustration is a new method for producing low-cost microfluidic devices using an original composite made of a polyurethane-based open cell foam (Bulpren PPI 90, Recticel) and a hyper-elastic silicon rubber (Dragon Skin FX Pro). From these materials, we are able to produce fluidic channels in a fully deformable chip. As an example, a blood typing protocol can be performed by moving manually a simple roller that induces a peristaltic effect upon a soft fluidic network (Fig 1-left).

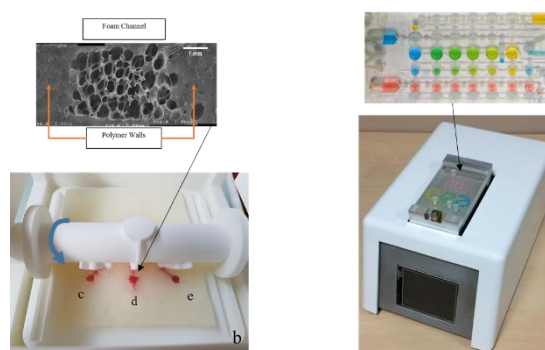


Figure 1: Foam based (left) and digital (right) portable microfluidic platforms using hyperelastic material

References

- [1] Unger M a, Chou HP, Thorsen T, Scherer a, Quake SR. Monolithic microfabricated valves and pumps by multilayer soft lithography. *Science*. 2000;288(5463):113-116. doi:10.1126/science.288.5463.113.
- [2] Wehner M, Truby RL, Fitzgerald DJ, et al. An integrated design and fabrication strategy for entirely soft, autonomous robots. *Nature*. 2016;536(7617):451-455. doi:10.1038/nature19100.
- [3] Pineda F, Bottausci F, Icard B, Malaquin L, Fouillet Y. Using electrofluidic devices as hyper-elastic strain sensors: Experimental and theoretical analysis. *Microelectron Eng*. 2015;144:27-31. doi:10.1016/j.mee.2015.02.013.

Biomimetic Capture of Odorant Molecules in a Microfluidic Device

E. Tulukcuoglu Guneri^a, T. Alava^a, Y. Fouillet^a, J. Casas^b

CEA LETI MINATEC Campus, Univ. Grenoble F-38054 Grenoble, France

^bInstitut de Recherche sur la Biologie de l'Insecte, IRBI CNRS UMR 7261 Faculté des Sciences, Université de Tours, F-37200 Tours, France

Key words: biomimetic, odorant uptake, olfactory mucus

Olfactory system demonstrates a remarkable capability of detecting extremely low concentrations of molecules at the range of parts-per-trillion and discriminating thousands of odor molecules [1, 2]. Following steps are involved in perceiving the odors via the olfactory system: lateral transport of airborne odorants molecules in the olfactory region, partial uptake at the air-mucus interface, diffusion through the mucus layer and potential interaction with mucus and finally binding to olfactory receptors triggering neuronal stimuli thereby leading to processing information and discrimination of odors.

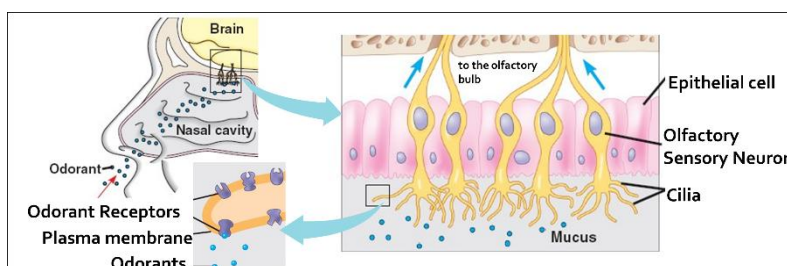


Figure 1: Scheme of a human olfactory system (image adapted from a figure in <http://bio1151b.nicernweb.net/Locked/media/cb49/smell.html>)

Olfactory system has been inspiring the development of systems for gas detection. For example, PDMS and agarose gel has been used to concentrate the gas molecules [3, 4] for subsequent detection analysis. A microfluidic system used water as a concentration layer mimicking the dimensions of the mucus layer in mammals [5]. Another biomimetic approach studied the role of the odorant binding proteins in odorant uptake using physiological conditions in human [6].

Despite its prevalence, the role physicochemical properties of olfactory mucus on olfaction is yet to be explored and olfactory mucus has not been a source of bio-inspiration. Here, we propose to develop a miniaturized the olfactory system recapitulating biomimetic olfactory mucus and nasal air flow using microfluidics. We are interested in studying spatial and temporal distribution of odorant uptake on the olfactory mucosa in which flow rate of the nasal air, solubility and diffusivity odorants in the mucus, thickness of the mucus, and potential interactions of odorant molecules with the components of the mucus are the key parameters effecting odorant uptake [7]. Hence, this study may uncover novel strategies for future sensor designs using bioinspired materials.

References

- [1] Keller A. et al, Human olfactory psychophysics., *Current Biology*, Vol 14, No 20, pp 875-878 (2004)
- [2] Bushdid C. et al, Humans Can Discriminate More than 1 Trillion Olfactory Stimuli, *Science*, Vol. 343, pp 1370-1372 (2014)
- [3] Olfaction-Inspired Sensing Using a Sensor System with Molecular Recognition and Optimal Classification Ability for Comprehensive Detection of Gases
- [4] Fujii S., Pesticide vapor sensing using an aptamer, nanopore, and agarose gel on a chip, *Lab Chip*, Vol 17, pp 2421-2425 (2017)
- [5] Piorek B, Free-surface microfluidics/surface-enhanced Raman spectroscopy for real-time trace vapor detection of explosives, *Analytical Chemistry*, Vol 84, pp 9700–9705 (2012)
- [6] Yabuki M., Dynamics of Odorant Binding to Thin Aqueous Films of Rat-OBP3. *Chemical Senses*, Vol 36, pp.659-671 (2011)
- [7] Hahn I. et al, A mass transport model of olfaction, *J Theor. Biol.* Vol 167, pp115-128 (1994)

Microfluidic standardization: a status

N. Verplanck^a and H. van Heeren^b

^a*Univ. Grenoble Alpes, CEA, Leti, DTBS, F-38000 Grenoble, France*

^b*enablingMNT, The Netherlands*

Key words: microfluidic, standardization, Microfluidic Association, ISO

1. Introduction

Standardization is key to reach maturity of a domain (reliable products, design guidelines, interoperability...) and helps R&D teams to reduce the time of development drastically.

During the last years, a general awareness of this has driven microfluidic stakeholders to work together (MFManufacturing project, ENIAC-JU, 2014-2017) on the standardization of microfluidics by formalizing standardization protocols, processes and guidelines in order to serve a wide range of users. [1] [2]

The consortium has initiated a new ISO working group [3] and initiated an International Microfluidic Association with over 75 interested parties from 19 countries to lead the future work.

2. Current agreement and future work

First, to enable interoperability of microfluidic devices and promote “plug and play” multiport interconnections, the group decided to define the size of the chip and the port pitch (grid of 1.5 mm). To simplify discussions between designers and users the group also defined a system for coding the ports. The next figure gives an example, where the microfluidic port positions in a 15*15 mm microfluidic building block are shown.

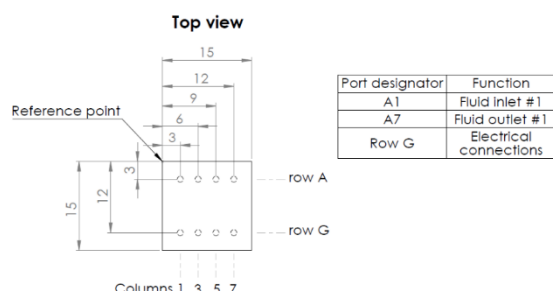


Figure 1: example of standard agreement 15 & 15 mm building block, with positions and coding of ports [1]

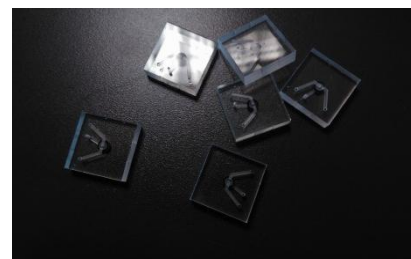


Figure 2: application of the standards to a pneumatic valve, developed by CEA-LETI

This initial step in standardization paves the way for the coming work on the standardization of flow control, test protocols (for product datasheets), modularity and interfacing.

References

- [1] H. van Heeren *et al.*, "Design Guideline for Microfluidic Device and Component Interfaces (part 1) v2", WhitePaper, <http://www.mf-manufacturing.eu> (2016)
- [2] H. van Heeren *et al.*, "Microfluidic standardization, status overview", MicroNanoConf. (2016)
- [3] "Interoperability of microfluidic devices: Guidelines for pitch spacing dimensions and initial device classification", IWA 23:2016, London, April 2016

Microfluidic devices and systems for bio-mimic approaches of stem cells

Y. Chen

Ecole Normale Supérieure, 24 rue Lhomond, 75005 Paris, France

Key words: Nanofabrication, Microfluidics, Automation, Stem Cells

Understanding and mimicking the in-vivo stem cell processes are active endeavor toward clinical and industrial applications.

By using nanofabrication and microfluidic techniques, we fabricated monolayer nanofibers as culture substrates and elastoplastic devices as tissue integration platforms for human induced pluripotent stem cells based assays. Functional cardiomyocytes and neurons were obtained on the monolayer nanofibers showing the expected electrophysiological behaviors and drug responses. An automatic system has also been developed for bio-mimic and long-term regulation of the stem cell differentiation and culture conditions.

Together, we have established a new paradigm for the future studies and developments of stem cell based assays, disease modeling, drug screening and regenerative medicine.

Finally, we believe that the concepts and the device manufacturing techniques developed in this work will also be useful for the exploration of microfluidic technologies in general.

Microcapsule fabrication by membrane emulsification

M. Maleki^a, K. Xie^{a,b,c}, E. Talansier^a, H. Bodiguel^a, M. Léonetti^a, C. de Loubens^a

^a *Univ. Grenoble Alpes, CNRS, Grenoble INP*, LRP, 38000 Grenoble, France*

^{*} *Institute of Engineering Univ. Grenoble Alpes*

^b *Aix-Marseille Université, CNRS, Centrale Marseille, M2P2 UMR 7340, 13451, Marseille, France*

Key words: Microcapsule, emulsion, microfluidics

Batch emulsification is a classic method to fabricate suspensions of microcapsules. However, size distribution and elasticity of microcapsules vary on several orders of magnitudes [1]. On the other side, microfluidic droplet generators allow a precise control of the size and mechanical properties on microcapsules [2], but the rate of production is very low. Membrane emulsification is a mean to fabricate an emulsion, or a dispersion of an aqueous (or oil) phase in an oil (or aqueous) phase [3]. This method overcomes the difficulties like inhomogeneous size distribution and mass production that the other methods face with them [4]. The objective of this study is to develop a method of membrane emulsification for the production of uniform microcapsules.

A membrane emulsification was performed to produce self-assembled microcapsules by emulsification of 0.25% (w/w) solution of chitosan in rapeseed oil with surfactant. The aqueous phase was introduced inside the oil phase through a flat disc membrane, which is positioned under a paddle stirrer, which provides detachment mechanism of droplets. The membranes have ring regular arrays of pores of 5, 10 and 20 microns diameter and 200 micros spacing between the pores. They are made by stainless steel and treated by a hydrophobic coating process in order to generate water to oil emulsion.

We show that membrane emulsification is a versatile and efficient method to produce suspensions of microcapsules whose the average diameter can be varied according to the process parameters (membrane, flow rates, agitation). This method can be optimized to get suspensions with size variation of less than 15%.

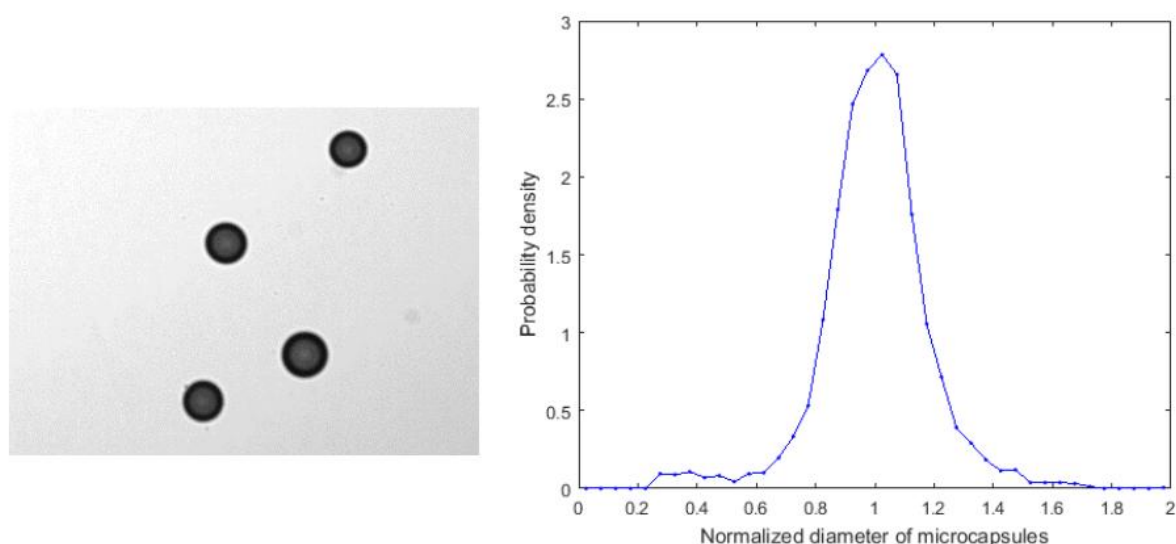


Figure 1: Microcapsules and the optimal probability density of size.

References

- [1] de Loubens, C., Deschamps, J., Georgelin, M., Charrier, A., Edwards-Levy, F., & Leonetti, M. (2014). Mechanical characterization of cross-linked serum albumin microcapsules. *Soft matter*, 10(25), 4561-4568.

- [2] Xie, K., De Loubens, C., Dubreuil, F., Gunes, D. Z., Jaeger, M., & Léonetti, M. (2017). Interfacial rheological properties of self-assembling biopolymer microcapsules. *Soft matter*, 13(36), 6208-6217.
- [3] Michael T. Stillwel et al, Stirred cell membrane emulsification and factors influencing dispersion drop size and uniformity, *Ind. Eng. Chem. Res.*, 46, 965 - 972 (2007)
- [4] Serguei R. Kosvintsev, Liquid-liquid membrane dispersion in a stirred cell with and without controlled shear, *Ind. Eng. Chem. Res.*, 44, 9323 - 9330 (2005)

Drying of a water-filled channel within an artificial leaf

B. Dollet^a, J. F. Louf^a, P. Marmottant^a

^a*LIPhy, UMR 5588 CNRS and Université Grenoble Alpes, France*

Key words: evaporation, permeable PDMS, artificial leaf

1. Introduction

The transport of sap in the vascular network of leaves is driven by evaporation at the surface of leaves, and it has been shown [1] that a relevant analogous physical system is a network of liquid-filled channels in a permeable polymer. As such, microfluidic systems made of PDMS are particularly suited. In our study, to understand how a leaf is susceptible to dry out if its supply of sap is stopped, we investigate the drying of water-filled channels, looking at the entry of air.

2. Experiments and results

We create a series of isolated channels of different widths in PDMS, using standard microfluidic techniques. All channels are open at one end and closed at the other hand. They are initially filled with water, then placed under a dry atmosphere. They progressively dry as a meniscus separating the still liquid-filled part and the newly dried part advances in the channel (Fig. 1). We record the motion of the meniscus with a camera, thereby measuring the rate of evaporation as a function of time. This rate decreases as the channel progressively dries, but surprisingly does not vanish at the moment where liquid water disappears in the channel. We rationalize our measurements by a model combining two contributions: (i) direct diffusion of water to the atmosphere through the thin layer of PDMS; (ii) diffusion between newly dried parts containing humid air and the dry atmosphere. In particular, we derive an asymptotic analytical prediction for the evaporation rate due to this latter process, using the fact that diffusivity of water is much lower in PDMS than in air. The data and the model are found to be in excellent agreement, thereby providing a good physical description for the drying-up of leaves. Preliminary results in more complex networks will also be presented.

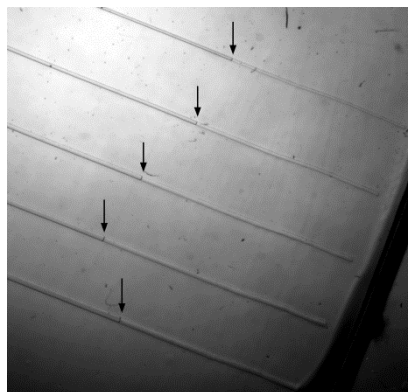


Figure 1: Drying channels (from top to bottom, 60, 80, 100, 120 and 140 μm in width). Arrows show the menisci.

References

[1] Noblin, Mahadevan, Coomaraswamy, Weitz, Holbrook & Zwieniecki, Optimal vein density in artificial and real leaves, *Proc. Natl. Acad. Sci.*, 105, 9140-9144 (2008).

Dropbox : an “off-the-shelf” microfluidic device for monodisperse emulsification based on a 3D-printed nozzle injector

A. Dewandre^a, Y. Vitry^a, B. Scheid^a

^a*Transferts, Interfaces et Procédés – Physique des Fluides, Université libre de Bruxelles*

Key words: droplet, dripping, microfluidics

Droplet generator is an important tool in many different fields, including complex emulsion and particle generation, drug delivery, protein dynamics, particle sorting and single cell analysis [1]. All the commercially available and most of lab-made droplet generators are based on a flow-focusing technology implemented in rectangular microchannels fabricated by lithography, and made in polydimethylsiloxane (PDMS), polymers or glass. This planar configuration has many limitations, mostly due to the contact between the walls of the chip and both phases at the junction, making an hydrophobic or hydrophilic coating necessary for water-in-oil or oil-in-water droplet generation, respectively.

Due to their axisymmetric flow, glass capillary devices on the other hand possess advantages for microfluidic applications, yet their widespread use is limited by the difficulty to implement this technology in an easy-to-use device. Co-flow systems have been set up using commercially available components, but these devices produce large droplets ($>100\ \mu\text{m}$) at low flow rate and lack the ability to generate small and monodisperse droplets ($<100\ \mu\text{m}$) at high flow rate that can be produced using a flow-focusing device. Furthermore, the centering of the capillary into an outer flow channel is challenging [2].

Glass capillary device for flow-focusing microfluidics droplet generation developed by Utada uses two circular capillaries inserted into a square outer flow channel, which greatly simplifies alignment and centering of the device. However, the restrictions necessary to obtain a focusing effect at the outlet of the inner capillary is obtained by pulling and breaking a glass capillary, a very “art-dependent” and not reproducible technique limiting the use of this design in microfluidic applications. Furthermore, the small space for the continuous phase between the glass capillary and the square channel limits the flow-rate, hence the high-throughput, in the droplet generation process.

Here we present a flow-focusing glass capillary device based on the alignment of two capillaries in a metallic chamber and the use of a 3D-printed nozzle injector. This configuration of the Utada design is fabricated using techniques that allow an industrial production of the device and a very easy-to-use experience for the end-user, while keeping all the advantages of the glass capillary flow focusing on the commercially available glass, polymer or PDMS chips.

We will present experimental results in various configurations (water/oil, oil/water, bubble/water, double emulsion) demonstrating the versatility of the device, and compare them to a force balance model developed to predict the size of the droplets.

References

- [1] Luoran Shang et al., Emerging Droplet Microfluidics, Chemical Reviews, 117, 7964-8040 (2017)
- [3] Serra et al., A Predictive Approach of the Influence of the Operating Parameters on the Size of Polymer Particles Synthesized in a Simplified Microfluidic System, Langmuir, 23, 7745-7750 (2007)
- [2] Utada et al., Monodisperse Double Emulsions Generated from a Microcapillary Device, Science, 308, 537-541 (2005)

Light propelled thermocapillary vessel

T. Dutour^a, E. Lorenceau^a, C. Picard^a

^aUniv. Grenoble Alpes, CNRS, LIPhy, 38000 Grenoble, France

Key words: interface, thermocapillarity, self-propulsion

Self-propelled micro-systems that consume energy available in their surrounding to ensure their motion often lead to spectacular collective behaviors that are not observed with systems at equilibrium. Biological systems are particularly well known to exhibit such behaviors. As an attempt to understand this collective behavior various mechanisms have been proposed to create simple self-propelled systems that may lead to complex collective interactions. The individual behavior of these objects, though, is intriguing in itself and constitute an essential prerequisite to investigate their collective behavior. In this framework, most of the studied systems rely on small bodies immersed into a liquid. The self propulsion of small bodies trapped at an interface have been much less considered. Nevertheless the so-called *soap-boat* constitutes a famous example where a small interfacial vessel is self propelled by a difference of surface tension generated by a flux of surfactant at the rear of the vessel [2]. Such a capillarity induced actuation is pedagogically interesting but works only in transient regime. The flux of surfactant is generally imposed and prevent the tuning of the actuation. Moreover the experimental characterization of the concentration field of surfactant, responsible for the vessel motion, is not straightforward.

In order to obtain a more controllable system, we recently developed a *sun-boat* based on a thermally induced difference of surface tension generated by a light source. From an energy conversion point of view the sun boat is a particular heat engine that relies on surface thermodynamics that is both surface tension differences and surface enthalpy differences. This type of propulsion, based on thermocapillarity and reminiscent of the thermal Marangoni effect, has recently been put forward to induce the self *rotation* of asymmetric microgears at an interface [3]. To be able to study *translational* motion we prepared small vessels few millimeter long that present a difference of radiation absorption coefficient between their bow and their stern. The light being uniformly shined perpendicularly to the surface, the difference of absorption results in a difference of temperature and subsequently a difference of surface tension that propels the vessel. The system can work in permanent regime as long as the heat transferred to the liquid is dissipated in the surrounding. The velocity of the vessel can easily be adjusted tuning the intensity of the light. Moreover the temperature fields at the interface that control the vessel motion, can be qualitatively measured by means of infra-red visualization. Experimental results allowed us to relate the permanent velocity of the vessel to the interfacial difference of temperature. The observed behavior suggests the presence of a transversal flow that significantly impact the heat transfer at the vicinity of the vessel and subsequently the velocity of the boat in a unexpected manner.



Figure 1: Infra-red view of a sun boat at a water/air interface (left) and schematic of the propulsion mechanism (right)

References

- [1] B. Irvin, *Energetics of the Marangoni instability*, Langmuir. **2** (1986)
- [2] E. Lauga et A. M. J. Davis. *Viscous Marangoni propulsion*, J. Fluid Mech. **705** (2012).
- [3] C. Maggi et al. *Micromotors with asymmetric shape that efficiently convert light into work by thermocapillary effects*, Nat. Commun. **6** (2015).

Drops, bubbles, etc ... (III)

Experimental study on acetone vapor as the tracer molecule for molecular tagging thermometry in gas microflows

Varun Yeachana, Christine Barrot, Lucien Baldas, Marcos Rojas-Cardenas, Stéphane Colin*
Institut Clément Ader (ICA), Université de Toulouse, CNRS, INSA, ISAE-SUPAERO, Mines-Albi, UPS, Toulouse
colin@insa-toulouse.fr

Molecular tagging, gas microflows, luminescence, phosphorescence

In recent years, gas flows in microdevices have become of particular relevance in several interesting microfluidic applications [1]. In these devices, the gas is subjected to rarefaction effects, and local thermodynamic disequilibria are manifested as velocity slip and temperature jump at the wall. Limited experimental data is available in this domain, particularly concerning local measurements of velocity and temperature [1, 2]. The Molecular Tagging Thermometry (MTT) technique has shown great potential to get local temperature data [2-5]. This technique introduces luminescent tracer molecules (such as acetone) in gas flows to map temperature profiles. In this study, preliminary experiments and analysis have been carried out to understand the light emission dependency of acetone with temperature.

The MTT setup can be divided into two distinct parts: (1) a gas circuit for flow seeding and control of operating conditions and (2) tagging and detection elements composed of heating elements, temperature sensors, and laser for molecular tagging, data acquisition and processing system. Experimental acquisition of the light intensity of pure acetone, excited at a wavelength of 310 nm, as a function of delay time, was carried out at pressures varying between 15,000 Pa and 1000 Pa and various conditions of temperature (20 °C, 34 °C, and 50 °C).

Analysis of the experimental data clearly indicates a dependency of light intensity and phosphorescence lifetime with temperature. This study is a step towards developing and implementing the molecular tagging thermometry (MTT) technique to map temperature profiles and to understand temperature jump at the walls in rarefied gas microflows.

Acknowledgements

This project has received funding from the European Union's Framework Programme for Research and Innovation Horizon 2020 (2014-2020) under the Marie Skłodowska-Curie Grant Agreement No. 643095, and from the Fédération de Recherche FERMAT (FR 3089).

References

- [1] Colin, S. (2012). Gas microflows in the slip flow regime: a critical review on convective heat transfer. *Journal of Heat Transfer*, 134(2), 020908.
- [2] Samouda, F., Colin, S., Barrot, C., Baldas, L., and Brandner, J., (2015). Micro molecular tagging velocimetry for analysis of gas flows in mini and micro systems. *Microsystem Technologies*, 21(3), 527-537.
- [3] Frezzotti, A., Si Hadj Mohand, H., Barrot, C. and Colin, S. (2015). Role of diffusion on molecular tagging velocimetry technique for rarefied gas flow analysis. *Microfluidics and Nanofluidics*. 19(6),1335-1348.
- [4] Si Hadj Mohand, H., Frezzotti, A., Brandner, J., Barrot, C. and Colin, S. (2017). Molecular tagging velocimetry by direct phosphorescence in gas microflows: correction of Taylor dispersion. *Experimental Thermal and Fluid Science*. 83, 177-190.
- [5] Fratanonio, D., Yeachana, V., Rojas-Cárdenas, M., Barrot, C. and Colin, S. (2017). Acetone and diacetyl phosphorescence at low pressures for molecular tagging velocimetry in confined rarefied gas flows. *Proceedings of 2nd International MIGRATE Workshop, Sofia, Bulgaria, MIGRATE-154814* 2017.

Dynamics and dissolution of bubbles in microchannels

J. Rivero-Rodríguez^a, B. Scheid^a

^a*Transferts, Interfaces et Procédés - Physique des fluides, Université Libre de Bruxelles*

Key words: Bubble dynamics, migration, mass transfer

This work focuses on the dynamics of a train of unconfined bubbles flowing in microchannels [1]. We numerically investigate the transverse position of a train of bubbles, its velocity and the associated pressure drop when flowing in a microchannel depending on the internal forces due to viscosity, inertia and capillarity. Despite the small scales of the system, the inertial migration force plays a crucial role in determining the transverse equilibrium position of the bubbles. Beside inertia and viscosity, other effects may also affect the transverse migration of bubbles such as the Marangoni surface stresses and the surface deformability. We look at the influence of surfactants in the limit of infinite Marangoni effect which yields rigid bubble interface. The resulting migration force may balance external body forces if present such as buoyancy, centrifugal or magnetic ones. This balance not only determines the transverse position of the bubbles but, consequently, the surrounding flow structure, which can be determinant for any mass/heat transfer process involved. We look at the influence of the bubble deformation on the equilibrium position and compare it to the inertial migration force at the centred position, explaining the stable or unstable character of this position accordingly.

We also investigate how the mass transfer is affected by the channel and bubble sizes, distance between bubbles, diffusivity, mean velocity, deformation of the bubble, the presence of surfactants in the limit of infinite Marangoni effects and the transverse position of the bubbles. We study the effects of the dimensionless numbers, specially the Pe number, which we vary among eight decades and identify four different regimes. These regimes can be classified by either the importance of the streamline diffusion or by the interaction between bubbles. For small Pe the streamline diffusion is not negligible as compared to convection whereas for large Pe , convection dominates in the streamline direction and, thus, crosswind diffusion becomes crucial to determine the dissolution through a boundary layer or of the remaining wake behind the bubbles. Bubbles interaction takes place for very small Pe number for which the dissolution is purely diffusive or for very large Pe numbers in which case long wakes eventually reach the next bubble. Transitions and asymptotic behaviours are finally explored.

Références

- [1] J. Rivero-Rodríguez and B. Scheid. Bubbles dynamics in microchannels : inertial and capillary migration forces. *Journal of Fluid Mechanics*, Accepted for publication :-, 2018.

Cavitating flow in microchannels : thermal effects and chemiluminescence.

D. Colombet^a, D. Podbevsek^b, G. Ledoux^b, F. Ayela^a

^aLEGI, Univ. Grenoble Alpes, CNRS, 38000 Grenoble, France.

^bILM, Université Claude Bernard Lyon 1, 69622 Villeurbanne, France.

Keywords: hydrodynamic cavitation, thermal-effects, chemiluminescence

Cavitating flows are usually found in many industrial applications. Cavitation corresponds to a phase change induced by pressure decrease below the saturated vapour pressure. This can be performed by acoustic waves, which is ultrasonic cavitation (USC), or by generating high speed flows, which is hydrodynamic cavitation (HC). Despite the large number of researches on that topic, many open questions are still unanswered. Among those questions, the role of the thermal effects coupled to the evaporation and to the condensation of bubbles clouds is very important for choosing model closure in numerical tools used for industrial design. A second question of interest is about the chemical reactions possibly induced by cavitating flows. During the collapse, the temperature inside the bubbles is suspected to reach a very important value ($T > 5000$ K). Sonoluminescence, which is light emission at the end of bubble collapse, has been observed both in USC as well as in HC experiments for a flow above an hydrofoil at the trailing edge [2]. That light emission, which is attributed to ionization of rare gas inside the bubble, demonstrates the violence of bubblecollapse which engenders sonochemistry because H_2O molecules may be broken into the reactive OH and H radicals. Even if it has been shown that some molecules can be broken in HC flows [1], there is up to now no consensus on the real efficiency of HC versus USC for wastewater treatments, nor any direct evidence of the formation of OH radicals in HC.

Hydrodynamic cavitation ‘on a chip’, that means inside microchannels equipped with a local constriction, appears to be an unrivaled method for the study of thermal effects and sonochemistry in HC. Experiments unavailable at macroscale become now possible, with devices working with low flow rates, able to handle a low amount of liquid and which can resist to an operating pressure of 20 bar. We have performed experiments through microdiaphragms, that has enhanced for the first time the thermal effects in water cavitating flows. For that purpose, the samples were mounted on a confocal microscope and thermosensitive nanoprobe functionalized with fluorescein were seeded into water. Such an approach has allowed us to draw a 2D mapping of the temperature in the liquid phase and to identify evaporation and condensation areas [3, 4]. Latest experiments have been performed to evaluate the possible production of OH radicals in HC. We have used an aqueous solution of luminol as the working fluid flowing through a microchannel. For the first time, chemiluminescence signal correlated to two-phase cavitating flows was quantitatively recorded [5]. The production of OH radicals is found to correspond to the end of the cavitating pocket, where vapour bubbles are expected to collapse and condense. Other innovative microfluidic experiments about laminar hydrodynamic cavitation will be also presented.

- [1] Zupanc M. et al., Removal of pharmaceuticals from wastewater by biological processes, hydrodynamic cavitation and UV treatment, *Ultrasonics Sonochemistry*, 20, 1104 (2013)
- [2] Farhat M. et al., Luminescence from hydrodynamic cavitation, *Proc. R. Soc. A*, 467, 591 (2011)
- [3] Ayela F. et al. , Experimental evidence of temperature gradients in cavitating microflows seeded with thermosensitive nanoprobe, *Phys. Rev. E* 88, 043016 (2013)
- [4] Ayela F. et al. , Thermal investigation of cavitating flows through microchannels, with the help of fluorescent nanoprobe. *La Houille Blanche*, 1, 103-108 (2015)
- [5] Podbevsek D. et al., Observation of chemiluminescence induced by hydrodynamic cavitation in microchannels. *Ultrasonics Sonochemistry* (2018) accepted article

Study of foams flows properties in model porous media

A. Mauray^a, M. Chabert^b, H. Bodiguel^a

^aUniv. Grenoble-Alpes, CNRS, Lab. LRP UMR 5520, F-38610 Gières, France

^bSolvay, Novacare, EOR, Singapore 138622

Key words: Foam, microfluidic, porous media

1. Introduction

In enhance oil recovery (EOR), to limit viscous fingering, foams are injected by co-injection of a gas and a solution of surfactants in porous media in order to improve oil recovery efficiency. This work focuses on foam transport mechanisms in model porous media using a heterogeneous micromodel made in NOA [1].

2. Results

We studied the transport properties of foam in a model porous medium. Direct measurements show that the pressure drop induces by the flow can be at $Ca=10^{-6}$ as high as 3000 times the pressure corresponding to water injected at the same injection flow rate. This ratio decreases with capillary number like foam flow in rocks [2,3]. An analysis of the preferential paths by direct observations shows that, for low relative gas flow rate, only a few paths are active. However, an increase of the capillary number or the relative gas flow rate leads to a homogenization of the flow in the medium. Thanks to different simple models of straight or wavy channels, we measure that the pressure drop induced by a single bubble follows two regimes.

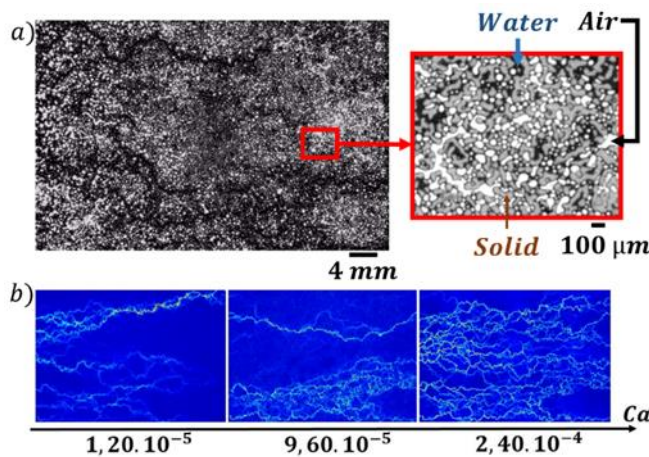


Figure 1. a) Photo of a foam transport in a porous medium. b) Maps of different preferential paths.

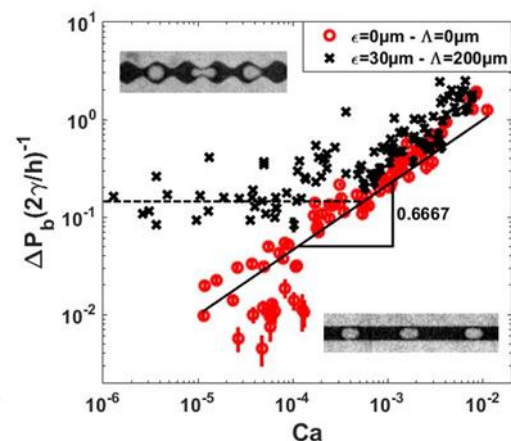


Figure 2. Evolution of the difference of pressure for a single bubble in straight and constricted microfluidic channel.

References

- [1] B. Levaché, A. Azioune, M. Bourrel, V. Studer, and D. Bartolo, *Lab on a Chip*, **12**, 3028-3031, (2012).
- [2] M. Lotfollahi, R. Farajzadeh, M. Delshad, A. Varavei, and W.R. Rossen. *Journal of Natural Gas Science and Engineering*, **31**, 184-197, (2016).
- [3] O. Gassara, F. Douarche, B. Braconnier, and B. Bourbiaux, *Journal of Petroleum Science and Engineering*, **159**, 588-602 (2017).

Whispering gallery mode yields intense acoustic streaming in sessile droplets

Antoine Riaud^{a,b,d}, Michaël Baudoin^a, Philippe Brunet^c, Jean-Louis Thomas^b, Olivier Bou Matar^a

^aInstitut d'Electronique, de Microélectronique et Nanotechnologie (IEMN), LIA LICs, Université Lille 1 and EC Lille, UMR CNRS 8520, 59652 Villeneuve d'Ascq, France

^b CNRS UMR 7588, UPMC Université Paris 06, Institut des NanoSciences de Paris (INSP), F-75005, Paris, France

^c Laboratoire Matière et Systèmes Complexes UMR CNRS 7057, 10 rue Alice Domon et Léonie Duquet 75205 Paris Cedex 13, France

^d Current affiliation : Université Paris Sorbonne Cité, INSERM UMR-S1147, CNRS SNC 5014, France. Equipe labellisée ligue contre le cancer

Key words: Acoustic streaming, computational fluid dynamics, caustics, surface acoustic waves

Acoustic streaming is a steady flow created by intense sound waves. It is an important phenomenon in digital microfluidics to expedite the mixing of sessile droplets. A typical configuration is to send trains of surface acoustic waves (SAW) beneath the droplet. These waves then radiate in the fluid and generate acoustic streaming. Despite the practical importance of this phenomenon, the detailed process between the radiation of the SAW and the acoustic streaming is unclear and most simulations rely on gross assumptions about the acoustic field in the droplet. In this study, we develop a first-principle numerical model to understand the relation between the radiated wave, the acoustic streaming force and the resulting flow field.

According to our simulations, the flow is driven by two types of ultrasonic caustics (i) volume caustics reflected from the droplet surface similarly to a concave mirror (not shown here) and (ii) surface caustics analog to a whispering gallery mode shown in figure 1.A. Remarkably, the surface caustics describe periodic orbits along the droplet surface and therefore remain coherent even after long fly times, whereas volume caustics become increasingly chaotic. Once the force term identified, we computed the flow pattern and compared it to experimental data (Fig. 1B). The good agreement supports that the acoustic field is accurately captured by the numerical model. Furthermore, the caustics physically correspond to the points where the flow is the most intense. Eventually, by tuning the liquid viscosity, we were able to vary the relative importance of surface and volume caustics: at low viscosity, surface caustics efficiently resonate and create a strong quadrupolar flow pattern (figure 1.B) whereas at high viscosity the volume caustics are stronger and yield a dipolar flow pattern (not shown here).

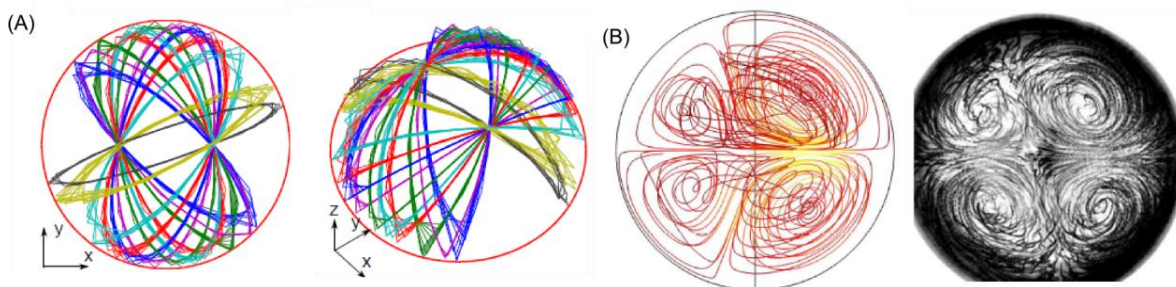


Figure 1: (A) Geometrical acoustic interpretation of the acoustic streaming in sessile droplets. The whispering gallery mode is represented here. The rays propagate along periodic orbits guided by the droplet surface. (B) Hydrodynamic flow (numerical result on the left and experimental PIV streamlines on the right).

In conclusion, we have developed first-principle algorithm to compute the acoustic field and acoustic streaming in sessile droplets. It unveils for the first time the existence of powerful caustics that concentrate most of the acoustic power and generate the streaming flow. This study paves the way to understand more complicated acousto-fluidic phenomena such as droplet displacement or atomization.

List of participants

- Abdorahim Marjan
- Alexandre Lucile
- Arauz Moreno Carlos
- Ayela Frederic
- Bancaud Aurélien
- Bodiguel Hugues
- Bottausci Frederic
- Bouriau Michel
- Brillouet Nicolas
- Brossard Rémy
- Brun-Cosme-Bruny Marvin
- Calmo Roberta
- Cappello Jean
- Cavaniol Charles
- Champougny Lorène
- Chateaux Jean-François
- Chaussavoine Igor
- Chevalier Caroline
- Colombet Damien
- Coron Charlène
- Cottet Jonathan
- Coupier Gwennou
- Davoust Laurent
- De Loubens Clement
- Delarue Morgan
- Descroix Stephanie
- Dewandre Adrien
- Di Leonardo Roberto
- Dollet Benjamin
- Elettro Hervé
- Elias Jinane
- Faivre Magalie
- Fattaccioli Jacques
- Fratzl Mario
- Fu Li
- Gue Anne-Marie
- Guneyusu Daniel
- Hadji Celine
- Hajji Ismail
- Harazi Maxime
- Hodaib Ahmed
- Issenmann Bruno
- Joseph Pierre
- Juel Anne
- Jullien Marie-Caroline
- Keita Camille
- Kerdraon Margaux
- Kleimann Pascal
- Krammer Thibault
- Lallart Adeline
- Lassalle Benedikt
- Le Blay Marine
- Le Gac Séverine
- Le Goff Anne
- Leblois Thérèse
- Lerisson Gaétan
- Liot Olivier
- Lorenceau Elise
- Maleki Mehdi
- Manczak Rémi
- Mansur Alexandre
- Marbach Sophie
- Marmottant Philippe
- Martin Elian
- Mauray Alexis
- Mcgraw Joshua
- Mekkaoui Samir
- Menezes Roberta
- Naillon Antoine
- Oseev Aleksandr
- Paliard Philippe
- Parent Charlotte
- Pascual Marc
- Picard Cyril
- Pierron Maxime
- Podgorski Thomas

- Pothier Arnaud
- Qiu Xiaoyu
- Rabaud David
- Rafaï Salima
- Reichert Benjamin
- Remy-Martin Fabien
- Renaud Louis
- Riaud Antoine
- Rivero-Rodriguez Javier
- Robert De Saint Vincent Matthieu
- Rodgar Majid
- Sasanpour Mehrzad
- Scaiola Davide
- Scorretti Riccardo
- Sepulveda Julian
- Serra Marco
- Sharma Preeti
- Siconolfi Lorenzo
- Constant Taindjis
- Taly Valerie
- Thomy Vincent
- Thupnot Thibaut
- Treizebre Anthony
- Truchet Marine
- Tulukcuoglu Guneri Ezgi
- Vauchier Claude
- Velasco Dandara
- Venzac Bastien
- Verplanck Nicolas
- Vilotte Alice
- Viovy Jean Louis
- Xie Kaili
- Yeachana Venkata

List of exhibitors

- **Amatek Vision Research**
Taindjis/Constant
- **Elveflow**
Fabien Cespro
- **Fluigent**
Thibaut Thupnot
- **Kloe**
Charlène Coron
Nicolas Brillouet

Author Index

- Achard Jean-Luc, 59
Alava Thomas, 60
Alexandre Lucile, 47
Aly Mohammed, 19
Andre C, 29
Ayela Frederic, 24, 71
- Bäumchen Oliver, 19
Baldas Lucien, 69
Barrot Christine, 69
Bartolo Denis, 18
Baudoin Michaël, 73
Bellayer Severine, 29
Benzaquen Michael, 19
Berthelard Romain, 42
Bizien Thomas, 15
Blaire Guillaume, 53
Blatché Charline, 30
Bocquet Lyderic, 39, 40
Bodiguel Hugues, 21, 22, 72
Bosco Francesca, 52
Bou Matar Olivier, 73
Bouchiat Vincent, 24
Bruckert Franz, 53
Brun-Cosme-Bruny Marvin, 57
Brunet Philippe, 73
- Calmo Roberta, 52
Cantat Isabelle, 9
Cappello Jean, 35
Cartellier Alain, 11, 12
Casas Jerome, 60
Caupin Frédéric, 42
Chabert Max, 72
Champougny Lorène, 27
Charlaix Elisabeth, 11, 12, 38
Chaussavoine Igor, 15, 28
Chavas Leonard, 15
Chen Yong, 62
Chiadò Alessandro, 52
Coasne Benoit, 21, 22
Coffinier Yannick, 29
Colin Stéphane, 69
Colombet Damien, 24, 71
Cottet Jonathan, 31
Courson Rémi, 30
Cugat Orphée, 53
- Dalmay Claire, 49
Dalnoki-Veress Kari, 19
Dargent Thomas, 29
Davoust Laurent, 59
De Loubens Clement, 8
Dean David, 39, 40
Decock Jérémy, 58
Dehaoui Amine, 42
Delaplace Guillaume, 29
Delarue Morgan, 48
Dellavalle Dominique, 54
Delshadi Sarah, 53
Dempsey Nora, 53
Descroix Stéphanie, 16, 17, 47
Devillers Thibaut, 53
Dewandre Adrien, 66
Di Leonardo Roberto, 33
Dollet Benjamin, 21, 22, 65
Du Roure Olivia, 35
Dubreuil Frédéric, 8
Duprat Camille, 35
Dutour Thomas, 67
- Eilstein Nathalie, 47
- Fattaccioli Jacques, 50
Ferrante Ivan, 17
Figarol Agathe, 25, 26
Fouillet Yves, 59, 60
Fowler Paul, 19
Fratzl Mario, 53
Fu Li, 41
- Garcia Léo, 25, 26
Garnier Philippe, 11, 12
Gines Guillaume, 55, 56
Gropplero Giacomo, 59
Gué Anne-Marie, 30
Guibourdenche Jean, 47
- Hadji Celine, 21, 22
Hallatschek Oskar, 48
Hatzikiriakos Savvas, 29
Hjeij Fatima, 49
Holt Liam, 48
Huerre Axel, 9
- Ilton Mark, 19

Issenmann Bruno, 42
 Jimenez Maude, 29
 Joly Laurent, 41
 Joseph Pierre, 13, 25, 26
 Juel Anne, 6
 Jullien Marie-Caroline, 9, 16, 27
 Kaynak Mehmet, 49
 Keita Camille, 58
 Kerdraon Margaux, 16
 Lallart Adeline, 11, 12
 Lalloué F., 49
 Lassalle Benedikt, 15
 Latargez Charlotte, 21, 22
 Laura Trapiella Alfonso, 47
 Le Blay Marine, 18
 Le Gac Séverine, 44
 Le Goff Anne, 36
 Lecarpentier Edouard, 47
 Ledoux Gilles, 71
 Lefrançois Stéphane, 15
 Leonetti Marc, 8
 Leroy Valentin, 27
 Liatimi Youssef, 15
 Lindner Anke, 35
 Liot Olivier, 25, 26
 Liu Yang, 17
 Loisel Catherine, 54
 Lorenceau Elise, 11, 12, 21, 22, 67
 Louf Jean-François, 65
 Lovera Andrea, 52
 Malaquin Laurent, 17, 47
 Maleki Mehdi, 63, 64
 Manczak Rémi, 49
 Mansur Alexandre, 20
 Marbach Sophie, 39, 40
 Marmottant Philippe, 65
 Mateo Tiphaine, 15
 Mauray Alexis, 72
 McGraw Joshua, 16, 19
 Menezes Roberta, 55, 56
 Merabia Samy, 41
 Mesdjian Olivier, 50
 Mingotaud Anne-Françoise, 25, 26
 Montillet Agnès, 54
 Moradi S, 29
 Naillon Antoine, 13
 Niguès Antoine, 39, 40
 Parent Charlotte, 59
 Picard Cyril, 38, 67
 Pierre Juliette, 27
 Podbevsek Darjan, 71
 Pothier Arnaud, 49
 Prat Marc, 13
 Qiu Xiaoyu, 24
 Raphaël Elie, 19
 Reichert Benjamin, 9
 Renaud Philippe, 23
 Riaublanc Alain, 54
 Riaud Antoine, 73
 Ricciardi Carlo, 23, 52
 Rivero-Rodriguez Javier, 70
 Rivetti Marco, 19
 Rojas-Cardenas Marcos, 69
 Rondelez Yannick, 55, 56
 Saada Sofiane, 49
 Sakai Kaori, 50
 Salez Thomas, 19
 Salmon Jean-Baptiste, 58
 Salsac Anne-Virginie, 36
 Scaiola Davide, 23
 Scheid Benoit, 70
 Schlenk Mathias, 58
 Sepulveda Julian, 54
 Sharma Preeti, 38
 Singh Lokendra, 42
 Siria Alessandro, 39, 40
 Socol Marius, 25, 26
 Stassi Stefano, 23, 52
 Taly Valerie, 55, 56
 Theodoly Olivier, 9
 Thiéry Juliette, 25, 26
 Thomas Jean-Louis, 73
 Thomy Vincent, 29
 Treizebre Anthony, 46
 Tsatsaris Vassilis, 47
 Tulukcuoglu Guner Ezgi, 60
 Valette Marion, 30
 Van Heeren Henne, 61
 Vargas Pablo, 17
 Venzac Bastien, 17
 Verhulsel Marine, 17
 Verplanck Nicolas, 61
 Vesperini Doriane, 36
 Viovy Jean, 47
 Viovy Jean-Louis, 17
 Xie Kaili, 8
 Yamada Ayako, 17
 Yeachana Varun, 69
 Zouaghi Sawsen, 29